JOURNAL OF PROPULSION AND POWER
Vol. 26, No. 4, July–August 2010

Review: Laser-Ablation Propulsion

Claude Phipps
Photonic Associates, LLC, Santa Fe, New Mexico 87508
Mitat Birkan
U.S. Air Force Office of Scientific Research, Arlington, VA 22203-1768
Willy Bohn
BohnLaser Consult, 70569 Stuttgart, Germany
Hans-Albert Eckel
DLR, German Aerospace Center, 70569 Stuttgart, Germany
Hideyuki Horisawa
Tokai University, Hiratsuka 259-1292, Japan
Thomas Lippert
Paul Scherrer Institut, 5232 Villigen PSI Switzerland
Max Michaelis
University of KwaZulu–Natal, Durban 4001, South Africa
Yuri Rezunkov
Sosnovy Bor, Leningrad Region, Russia
Akihiro Sasoh
Nagoya University, Nagoya 464-8603, Japan
Wolfgang Schall
71111 Waldenbuch, Germany
Stefan Scharring
DLR, German Aerospace Center, 70569 Stuttgart, Germany
and
John Sinko
Kratos Defense and Security Solutions, Inc., Huntsville, Alabama 35805

DOI: 10.2514/1.43733

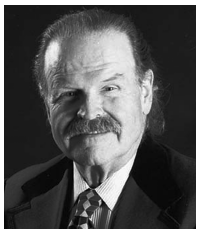

Claude Phipps earned B.S. and M.S. degrees from Massachusetts Institute of Technology and a Ph.D. from Stanford University in 1972. He worked in the Inertial Confinement Fusion Program at Lawrence Livermore Laboratory for two years and, since 1974, as a Senior Research Staff Member in the Advanced Optical Systems Group at Los Alamos (LANL). There, he conducted a research program on mechanical and thermal coupling of pulsed lasers to targets using high-energy-laser facilities in the United States and United Kingdom, and he developed a model for vacuum laser impulse prediction. From 1994 to 1995, he was Associate Director of the Alliance for Photonic Technology at LANL. In 1995, he formed Photonic Associates, which is devoted to applications of laser space propulsion. He is the author of 110 papers and 40 invited talks and an editor of a book on laser ablation, and he has been the organizer and chair of seven symposia on high-power laser ablation. He is a Governing Board Member of the American Institute of Beamed Energy Propulsion, which gave him its lifetime achievement award in 2005. He is a Senior Member of the AIAA.

Mitat A. Birkan is the program manager of the Space Propulsion and Power Program at the U.S. Air Force Office of Scientific Research. He is responsible for the U.S. Air Force basic research program in space propulsion, ensuring the excellence and relevance of a broad research portfolio. The research includes electric propulsion, chemical rocket propulsion, and plume signature characterization and contamination. Dr. Birkan is widely known for his contributions in the areas of two-phase combusting flows, perturbation techniques, and mathematical modeling of detonations and explosions. Dr. Birkan has authored more than 25 technical papers in the areas of combustion and space propulsion.

Received 10 February 2009; revision received 22 October 2009; accepted for publication 9 November 2009.

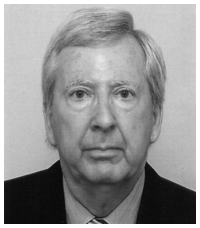

Willy Bohn began the study of physics at the University of Liège and finished his M.S. degree in physics at the Technical University of Aachen in 1964. After working in plasma physics and fusion research, he became involved in nonequilibrium plasma flows in the early 1970s and subsequently entered the field of flow lasers, with emphasis on CO and CO_2 gas dynamic lasers at the DLR, German Aerospace Center. He obtained his Ph.D. from the University of Stuttgart in the mid-1980s and worked several times in the United States: in particular, at Princeton University, Bell Laboratories, Holmdel, and the U.S. Air Force Research Laboratory. He was appointed Deputy Director of the DLR's Institute of Technical Physics in 1986 and then Professor and Director in 2000. He retired from this position in March 2008 and has worked since then as a Consultant. During his career he published more than 150 papers and applied for more than 20 patents in the areas of high-energy-laser (chemical, electrical, and solid-sate) interaction and nonlinear optics. He is a Senior Member of the AIAA.

Hans-Albert Eckel received a Ph.D. degree in physics from the University of Kaiserslautern in 1996. He is Head of the Studies and Concepts section of the DLR, German Aerospace Center's Institute of Technical Physics, where he has worked since 1997. His research areas include high-power lasers, atmospheric propagation, laser–matter interaction, and airborne- and space-related laser applications. Since 1998, Dr. Eckel has been engaged in the assessment of future applications for laser propulsion.

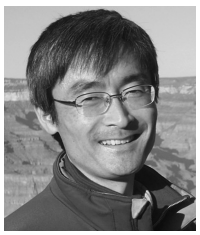

Hideyuki Horisawa is a Professor in the Department of Aeronautics and Astronautics, School of Engineering, Tokai Univerisity, where he received his Ph.D. in plasma-assisted combustion in 1993. Then he became an Assistant Professor in the Department of Precision Engineering at Tokai University, where his study extended to low-power plasma sources and laser/plasma processing of materials. In 2001, he became an Associate Professor in the Department of Aeronautics and Astronautics at the same university, where he extended his field to space propulsion applications, including electric propulsion and laser propulsion systems. In 2007, he joined Prof. Cappelli's group as a Visiting Professor of mechanical engineering at Stanford University, where his research further extended to microdischarge applications. He is a Senior Member of the AIAA.

Thomas Lippert studied chemistry at the University of Bayreuth. He was a Postdoctoral Fellow at the National Institute of Materials and Chemical Research. After that, he moved to Los Alamos National Laboratory, where he also became a Technical Staff Member. In 1999, he became a Senior Scientist at the Paul Scherrer Institut, where he currently heads the Materials group. In 2002, he received his Habilitation at ETH Zürich in physical chemistry and became Senior Lecturer (Privatdozent). The research of Dr. Lippert is focused on the interaction of photons with materials and the development of materials for laser applications. Dr. Lippert has published more than 190 papers, delivered more than 85 invited talks, and organized four international conferences, and he is a Member of the Editorial Boards of three journals.

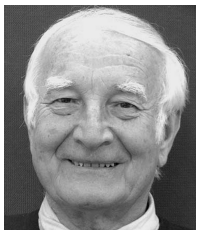

Max Michaelis received his D.Phil. from Oxford University in 1973. He has taught physics at the University of Natal for a quarter of a century. His laser group researched such topics as the refractive fringe diagnostic of laser-produced plasmas and shock waves in air. They invented two new gas lenses: the colliding shock lens and the flame lens. An atmospheric lidar was installed and operated for several years. At Pelindaba (Atomic Energy Commission) laser propulsion experiments were conducted with a kilowatt CO_2 laser. Similar experiments are planned at the National Laser Centre. Dr. Michaelis originated simulations of physical phenomena such as shock waves with magnetic pucks. A coupled-oscillations toy known as the Maxnet was marketed.

Yuri Rezunkov graduated from Leningrad Polytechnic Institute in 1977. He holds an Sc.D. He has published over 70 scientific papers on laser physics, including such topics as laser radiation propagation through the atmosphere, laser propulsion, and phase conjugation as applied to a laser beam control system. His publications are devoted to solving such problems as increasing of the delivery efficiency of laser energy through the atmosphere on the basis of the development of laser beam control techniques, development of the efficient laser propulsion engines, and laser systems to control lightning. At present, Dr. Rezunkov concentrates his research in the development of picosecond CO_2 lasers for application of the lasers in the field of monitoring in new materials, environment, and defense.

I. Introduction

LASER ablation propulsion (LAP) is a major new electric propulsion concept with a 35-year history. In LAP, an intense laser beam [pulsed or continuous wave (CW)] strikes a condensed-matter surface (solid or liquid) and produces a jet of vapor or plasma. Just as in a chemical rocket, thrust is produced by the resulting reaction force on the surface. Spacecraft and other objects can be propelled in this way. In some circumstances, there are advantages for this technique compared with other chemical and electric propulsion schemes. It is difficult to make a performance metric for LAP, because only a few of its applications are beyond the research phase and because it can be applied in widely different circumstances that would require entirely different metrics. These applications range from milliwatt-average-power satellite attitude-correction thrusters through kilowatt-average-power systems for reentering near-Earth space debris and megawatt-to-gigawatt systems for direct launch to low Earth orbit (LEO). Table 1 indicates qualitative metrics for LAP.

Table 1 [1–4] assumes an electric laser rather than a gas-dynamic or chemical laser driving the ablation, to emphasize the performance as an electric thruster. How is it possible for moderate laser electrical efficiency to give very high electrical efficiency? Because laser energy can be used to drive an exothermic reaction in the target material controlled by the laser input, and electrical efficiency only measures the ratio of exhaust power to electrical power. This distinction may seem artificial, but electrical efficiency is a key parameter for space applications, in which electrical power is at a premium.

The laser system involved in LAP may be remote from the propelled object (on another spacecraft or planet-based), for example, in laser-induced space-debris reentry or payload launch to low planetary orbit. In other applications (e.g., the laser–plasma microthruster that we will describe), a lightweight laser is part of the propulsion engine onboard the spacecraft.

II. Benefits, Scope, and History

A. How These Benefits are Achieved

Variable I_{sp} is achieved by adjusting laser intensity on the target, by changing the focal-spot area and laser-pulse duration, which causes exhaust velocity to vary across the range from chemical reactions (approximately, $I_{sp} \leq 500$ s) [4] to much higher values (3500–5000 s) [2]. This is because $v_E = (2kT_i/m_i)^{0.5}$ and 10,000 K ion temperatures T_i can easily be created with a laser pulse. In short, I_{sp} is only a matter of intensity [5]. Thrust can be varied independently of I_{sp} by changing the laser-pulse repetition rate. Tens-of-kilosecond specific impulses are possible using current laser technology: for example, $I_{sp} = 8.3\text{E}4$ s at $T = 1\text{E}8$ K in inertially confined fusion [6] (although lasers required to do this are currently too massive to be practical for a space vehicle).

Energy-use efficiency for a flight is strongly improved by constant-momentum exhaust-velocity profiles [7], which require variable I_{sp}, and this is extremely difficult to achieve with chemical jets.

Akihiro Sasoh obtained a Ph.D. from the University of Tokyo in steady-state applied-field magnetoplasmadynamics thrusters in 1989. He has been involved in nonchemical (that is, electric and laser) propulsion and compressible fluid dynamics, including shock waves, at the University of Tokyo, Nagoya University, and Tohoku University. He is currently a Professor in the Aerospace Department. He is an Associate Fellow of the AIAA.

Wolfgang Schall received the Diplom. degree in aeronautics and astronautics from the University of Stuttgart in 1968 and an M.S. in that field from the University of Washington in 1969. In the same year, he was appointed Research Scientist at the Institute of Plasmadynamics of the Deutsche Forschungs- und Versuchsanstalt für Luft- und Raumfahrt, which later became the DLR, German Aerospace Center's Institute of Technical Physics. He worked in the fields of magnetoplasmadynamics propulsion and, later, gas and chemical lasers. He was head of the group of chemical oxygen iodine lasers. Since 1999, he has participated in work on laser propulsion. In 2006, he retired from DLR.

Stefan Scharring studied physics at the University of Freiburg, supported by a scholarship from the German National Academic Foundation. After his Diplom. thesis on infrared spectroscopy with polymer layers for environmental applications, he dedicated several years of research to biophotonics at the Fraunhofer Institute and the German Weather Service. Since 2006, he has worked on pulsed laser propulsion with parabolic nozzles at the Institute of Technical Physics of the DLR, German Aerospace Center. A main topic of his research is spatially resolved analysis of impulse coupling and steering issues of laser-propelled free flights. Currently, he is preparing his Ph.D. thesis at the University of Stuttgart.

John Sinko graduated from Furman University with a B.S. in chemistry and mathematics (2003) and from the University of Alabama in Huntsville with an M.S. in physics (2005) on laser-ablation propulsion with liquid propellants and with a Ph.D. in physics (2008) on propellants and low-fluence models for laser-ablation propulsion. He currently works for Kratos Defense and Security Solutions, Inc. His research interests include fiber-optic sensors, laser ablation, and laser propulsion. He is a Member of the AIAA.

Table 1 Laser-ablation propulsion performance metrics [1–4]

Parameter	Value
Thrust-to-mass ratio	High (15 N/kg)
Thrust	Scales linearly with laser power
Thrust density	High (8E5 N/m^2)
Electrical efficiency	Very high (>100%)
Specific impulse	Low to Very high ($200 < I_{sp} < 3100$ s
Main benefit	Very high electrical efficiency, I_{sp}
Main limitation	40–60% laser electrical efficiency; more than newton-level thrust not yet demonstrated

For ground-based laser applications, the thrust-to-weight ratio is much higher than in electric propulsion, because the power production source remains on the ground. High specific impulse allows for high payload fractions m/M.

In self-contained laser propulsion engines, high-pressure or cryogenic fuel tanks, and high-power gas-driven turbopumps, nozzle cooling systems and the like are eliminated and replaced by relatively lightweight diode or diode-pumped fiber lasers. Because fiber lasers are efficient distributed systems with large surface-to-volume ratios, cooling of the laser itself is not a difficult problem up to the kilowatt-power, newton-thrust level. For larger thrust, with the technology available today, chemical rockets are still the best choice. But within this range, spacecraft with laser engines will be more agile. Vehicle specific mass on the order of 10 N/kg has been demonstrated [3]. For flight within the atmosphere, polymer propellants cause insignificant pollution.

The laser installation and power transmission unit for large systems on the ground constitute a considerable investment. However, since they can remain at a place where they are easily serviceable, they can be built more inexpensively, without space qualification.

Laser thrusters have demonstrated thrust density [8] on the order of 800 kN/m^2, because thrust is arising from a spot with an area equal to that of the laser focus. This is important in comparison with the much larger throat-area-to-thrust ratio of ion engines.

In systems intended for direct launch to LEO using a launch frequency of about five per day, the cost/kilogram delivered to LEO is dramatically reduced from present costs to as little as \$300/kg [9] for both chemical and laser launches (see Sec. VI.C). This launch frequency is not practical for chemical systems, but would be as easy as skeet-shooting for a laser launcher. The cost reduction comes about from spreading fixed equipment amortization and labor costs, the cost of ground-based electrical energy itself being only \$0.03/MJ.

Admittedly, some aspects of the claimed advantages are conceptual, in the sense that they remain to be demonstrated. However, those that have been demonstrated [e.g., laser–plasma thrusters [4] (Sec. V.A) and the more recent flights of the 1.5 N, 6 kW aerospace laser propulsion engine in the laboratory [8] (Sec. V.E)] indicate an exciting future for the technology.

B. Scope of This Review

Since our subject is laser-ablation propulsion, our scope does not include pure-photon propulsion (such as the elegant work of Bae [10]), except as we consider it to set the context for the evolution of the field beginning from photon propulsion in the next section. Because this paper treats propulsion by laser ablation, we mainly consider solid and liquid propellants. The work of Mead et al. [3] concerns aerodynamics and laser heating of gases rather than ablation (although ablation of the flyer itself currently plays a role, making analysis extremely complicated), the ultimate goal being to ablate nothing during transit through the atmosphere. However, it is still mentioned in Sec. V.D in the context of space flight, in which polyoxymethylene (POM) ablators will play a role. A complete treatment of so-called lightcraft, including theory both in atmosphere and vacuum, would be a different review. In the same spirit, we do not consider inertial confinement fusion except as a reference point in some plots. This review is primarily applications-oriented, although sufficient basic theory to understand LAP is provided.

C. Laser Propulsion: Early Historical Background

The idea to send a beam of light to a distant location and use its energy or its momentum has been around since antiquity, long before the laser was invented. Archimedes's mirrors reflecting sunlight and focusing it onto the Roman fleet of Commander Marcellus off the coast of Syracuse in 214 BC is the best-known example. True story or mere myth, the interesting point is that this story has persisted over more than 2000 years, demonstrating the attractiveness of such a capability. The first more-seriously-documented approaches to the application of directed light beams are found in the publications of the astronautic visionaries of the 20th century. In the years 1923 and 1924, the Russian pioneers Fridrikh Tsander [11] and Konstantin Tsiolkovsky [12] (Fig. 1) and, independently, the German Hermann Oberth [13] (Fig. 2) mentioned the idea of propulsion by light pressure, leading to the concept of light, or solar, sail. However, the Russian work was virtually unknown to the West until the 1930s, when rocket technology had developed through the independent efforts of Oberth in Germany and Goddard [14] in the United States. The early space-flight pioneers not only recognized the potential of liquid- and solid-fuel rocket propulsion to escape the Earth's gravity for interplanetary missions (moon and Mars), but they also realized its inherent limitations when it comes to interstellar voyages: a rocket will not be able to contain enough fuel to sustain its propulsion for the length of an interstellar mission. The only way out of this dilemma is to supply the rocket with energy from a fixed base, using electromagnetic beams. It was Eugen Sänger of Germany who proposed [15] in 1953 that a different type of propulsion concept would be

Fig. 1 F. Tsander (left) and K. Tsiolkovskii (right).

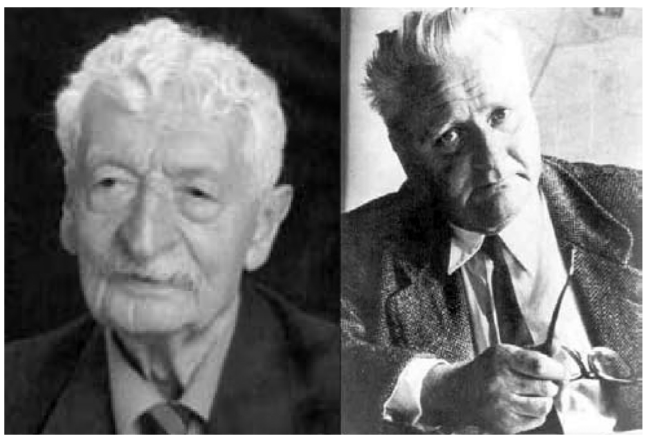

Fig. 2 H. Oberth (left) and E. Sänger (right).

needed for interstellar missions: i.e., the photon rocket. Since the laser was not invented at that time, Sänger envisioned photonic propulsion based on the continuum radiation of a hot plasma generated by a fission reactor placed at the focal point of a large reflector. The subsequent radiation pressure was supposed to give the necessary momentum to the reflector structure. Because of confusing the ionic with the nuclear charge number of uranium, Sänger overestimated the radiation pressure of such a plasma by four orders of magnitude. However, this mistake at a time when plasma physics was still in its infancy does not diminish the visionary value of his approach. Years later, after the invention of the laser in 1960, Sänger [16] modified the concept, as schematically shown in Fig. 3; he suggested a nuclear-pumped gas laser to provide the necessary radiation pressure. As an even more futuristic alternative, he considered a fusion reactor (still under development) and a matter–antimatter annihilation reactor, which is still more science fiction than reality.

The photonic propulsion scheme using a nuclear-pumped gas laser was revisited by the 1984 Physics Nobel Prize Laureate Carlo Rubbia at an Association Aéronautique et Astronautique de France meeting in Versailles in 2002. In this talk, Rubbia developed the idea to use a few kilograms of Americium 242 as the energy source for a 3 GW laser [17].

It took decades before a photonic propulsion concept (the lightsail) was actually realized. An advanced lightsail material was tested with high-power CO_2 lasers in 2000 at the Laser-Hardened Materials Evaluation Laboratory facility of the Wright-Patterson Air Force Base [18]. At the DLR, German Aerospace Center in Braunschweig, a large solar sail [19] (Fig. 4) was developed in the same year. Just recently, ESA showed a resurgence of interest in sailcraft and awarded the Luxembourg company LuxSpace and its partners a two-year project for solar sail materials in April 2008. This may be another starting point for the dream of caravelles in space to be realized.

Some years later, Georgii Marx, the head of Physics at the Roland Eotvos University in Budapest, wrote a short but seminal paper in *Nature* [20] in which he derived the surprising conclusion that though the instantaneous and total efficiencies of laser energy transfer start at zero, they reach around 42 and 67%, respectively, at half the speed of light and reach 100% at the speed of light itself.

Marx's [20] paper was followed a year later in the same journal by a highly critical analysis of his work by J. L. Redding [21]. Redding pointed out that Marx's [20] efficiency calculations did not take into account the laser energy stored in the space between the laser station and the spacecraft. According to Redding [21], a correction factor ought to be included that would reduce the Marxian efficiencies by half at $c/2$ and to zero at the speed of light itself.

It took a quarter-century for Marx's [20] work to be justified by Simmons and McInnes, writing in the *American Journal of Physics* [22]. They pointed out that provided one considers retarded time (i.e., spacecraft time) rather than terrestrial time, the Redding correction

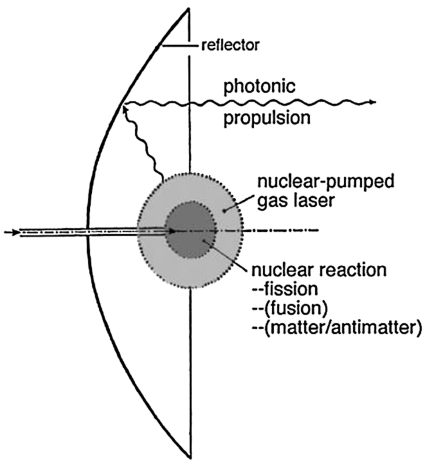

Fig. 3 Illustration of Sänger's photonic propulsion.

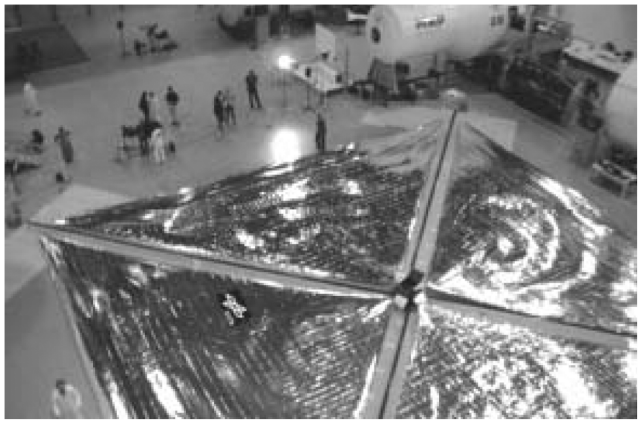

Fig. 4 Solar sails at DLR Braunschweig (see [4]).

drops away. Simmons and McInnes rederived one of Marx's most valuable equations. The relativistic velocity attained depends on the Marxian energy quotient Pt/Mc^2, which is the ratio of laser output energy to the spacecraft mass expressed as Mc^2.

Wolfgang Möckel was chief of the Advanced Propulsion Division at NASA Glenn Research Center at Lewis Field when he initiated research into advanced propulsion. In a seminal paper [23], Möckel laid down the basic equations for nonchemical propulsion. He was the first scientist to realize that, whereas almost unlimited exhaust velocities are possible for laser propulsion, the highest exhaust velocity is not necessarily the best. Most of the energy might go into the plume rather than the spacecraft.

D. Laser-Ablation Propulsion: A More Practical Concept

Pure-photon pressure is minute: the momentum-coupling coefficient for pure radiation reflecting off a polished surface is

$$C_m = 2/c = 6.7 \text{ nN/W} \tag{1}$$

and a 10 kW laser would produce a thrust of only 67 μN.

To get useful thrust levels, we require a very-high-power laser source or enhancement by a secondary physical phenomenon (such as thermal transpiration in low-pressure gas around the edges of the blades in a Crookes radiometer, which move in the opposite direction from that done in photon propulsion) or laser-induced surface ablation, which is the main subject of this paper.

The coupling coefficient due to laser-induced ablation of common materials can be $C_m = 100$ N/MW to 10 kN/MW, which is four to six orders of magnitude larger than the Eq. (1) value. In this sense, until gigawatt lasers are developed, perhaps in the next two decades, ablative propulsion is the only practical solution to achieving useful thrust from photons.

The paradigm shift in laser propulsion technology occurred in 1972, when Arthur Kantrowitz (Fig. 5) introduced and clearly formulated the idea [24] of ablative laser propulsion: a high-power laser beam focused onto the surface of a material can evaporate and even ionize part of that material, generating a specific impulse much higher than expected from classical chemical rockets.

Also in 1972, a first report by Pirri and Weiss [25] was published on fundamental experiments with steady-state and pulsed ablation in a parabolic reflector.

E. Pulsed-Laser-Ablation Propulsion Overview

In steady-state (CW) laser thrusters, high radiation intensity must be maintained for the continuous heating of the propellant flow to the plasma state. Because of the high breakdown intensity of gaseous propellants for continuous propellant flow even with megawatt CW laser power, only small plasma zones can be maintained. In contrast, high intensities over larger cross sections can easily be provided with medium-size pulsed lasers. Very simple configurations are possible for the ablation of solid propellants. Pulsed laser ablation can be used

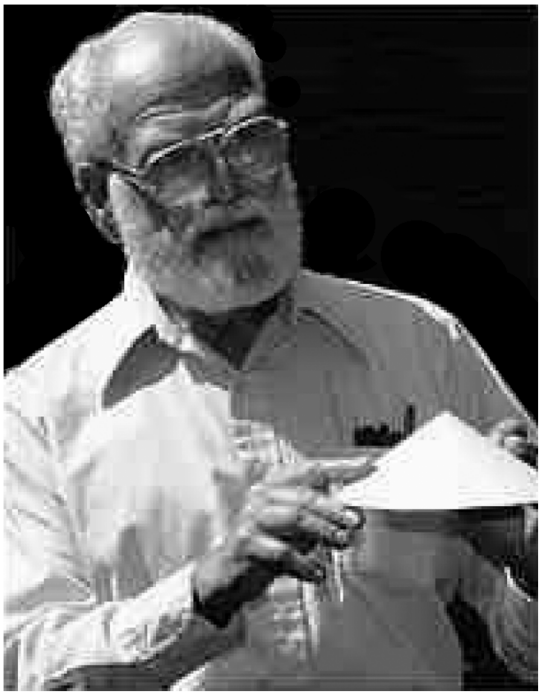

Fig. 5 A. Kantrowitz.

for propelling craft in multiple environments, each with its specific requirements for C_m and I_{sp}.

After a theoretical analysis by Bunkin and Prokhorov [26], scaling experiments with different concentrators for air breakdown started in Russia (Ageev et al. [27] in 1980). In 1984, results in the United States up to that year were reviewed by Glumb and Krier [28]. A major limitation for further progress at that time was the lack of lasers with sufficient power and stability. After a new initiative of the U.S. Air Force Office of Scientific Research and NASA, the first free flight of a 1997 laser rocket design by Myrabo et al. [29] resulted in a record flight height of 72 m in 2000 [30] (see Sec. V.D). Delrin® (polyoxymethylene, or POM) was used as the ablating propellant and still remains a most promising monopropellant. After Myrabo et al.'s [29] first successful flight experiments, similar investigations were reported from other countries (Russia in 1998 [31], Germany in 1999 [32], and Japan in 2001 [33]). Analysis of the possibilities and the requirements for early introduction of laser propulsion for space flight was carried out in 1994, when it was realized [9] that the introduction of laser propulsion into a well-established propulsion economy can only start in small steps, demonstrating the credibility of this new technology. So the first step was the development of laser-ablative microthrusters for attitude control and stationkeeping [34].

A special application of pulsed ablative laser propulsion was suggested by Schall [35] in 1990 and, later, Kusnetsov and Yarygin [36] in 1994. The propulsive effect of ablating a fraction of the debris itself can be used to deorbit space debris. Whereas these proposals relied on a space-based laser, Phipps et al. [37] worked out this idea for a ground-based system, called Orion (see Sec. VI.C).

Laboratory-scale wire-guided flight tests and tests of devices for measuring mechanical impulse and I_{sp} have been made for many different thruster geometries. The most simple is, of course, a flat plate, as is realized in the laser–plasma microthruster [34] (see Sec. V.A). If a beam concentrator is used, it can also function as a gas-dynamic nozzle. The simplest configuration is a cone or a paraboloid [27] or a matrix of paraboloids [31]. A more complex geometry was developed by Mead et al. [3]. Their concentrator had a ring shape around a central peak with parabolic contour, producing a ring line focus and serving, at the same time, as a plug nozzle. A different concept was followed by Sasoh [33] (see Sec. V.B). He placed the whole craft inside a tube, as in a cannon, to use the increase in gas pressure from the breakdown at the stern of the vehicle. If a long laser pulse at a high repetition frequency is radiated from behind into a thrust chamber, the light must pass through absorbing ablation products. To avoid premature absorption, Ageichik et al. [38] reflect the radiation sideways into the thrust chamber along its circumference. Their design is suitable for both pulsed and CW laser propulsion [8].

An important factor in the improvement of performance figures of merit and of ablation efficiency is choosing an appropriate propellant. In volume absorbers, i.e., polymeric materials, the incident light can penetrate deeply into the propellant material and liberate a substantial mass fraction for each laser pulse. This increases C_m and thrust. Because of the inherent inverse connection of C_m to the I_{sp} (Sec. III), exhaust velocity remains low. In contrast, surface absorbers, i.e., metals, liberate very little material with high I_{sp} at correspondingly low thrust. Within certain ranges, propellants can be designed to a desired performance criterion by blending materials with different absorption properties and mass, as shown by different groups [39–41]. A side effect can be the use of an exothermic reaction to substantially enhance the coupling efficiency [31,42,43]. Although liquid propellants were previously not suitable for space propulsion purposes because of splashing, improvements in momentum coupling can be achieved by special design of the ablation target [44]. Splashing is to be avoided for space applications because it preferentially channels incident laser energy into low-velocity ejecta and causes unacceptable spacecraft contamination. Yabe et al. [45], for instance, used metal targets with an overlying liquid film (water) to significantly increase C_m in terrestrial and airborne vehicle propulsion applications (see Secs. IV.B and VI.B). The drawback of extremely low I_{sp} and ablation efficiency has been overcome with transparent [46] or highly viscous liquids, and now I_{sp} up to 10,000 s appears realistic [47] (see Sec. IV.B).

F. Operating Range of Laser-Ablation Propulsion

Figure 6 shows a collection of published C_m vs I_{sp} data for different propellants [2,4,9,15,40,44,47–60]. Laser-pulse characteristics, wavelengths, and target materials are detailed in the references. Ablation efficiencies $\eta_{ab} > 1$ for the data shown can result from an exothermic reaction and from experimental error in measurements of p and I at very high intensity. It can also arise from propellant combustion in air if only the mass of the ablation fuel (and not the air consumed in combustion) is considered in measurements of I_{sp} (see Secs. III.A and IV.C.2). The superiority of polymeric propellants with additives is evident from their broad performance range. At the high end of I_{sp} in Fig. 6, relativistic effects play an increasing role and have been taken into account.

For a launch from Earth to space, $I_{sp} > 600$ s is highly desirable for delivering useful mass to orbit, and a C_m value of around 400 N/MW is optimum [60]. Chemical rockets are limited by achievable combustion temperatures to I_{sp} values on the order of 500 s. Currently, electric propulsion concepts lack the thrust-to-mass and thrust-to-power ratios required to launch from Earth. LAP is attractive because of the ability to have the power source separate from the thruster, which permits direct launch from Earth. Because I_{sp} is just a matter of intensity (see Sec. III.A), LAP can achieve a broad range of I_{sp} in onboard thrusters, to match requirements ranging up to those of long interplanetary or interstellar missions.

III. Theory of Momentum Generation

In this section, we will review the basic theory of laser-ablation propulsion. Throughout this section, our interest in reviewing analytical results extends only so far as to enable predictions of laser-ablation variables that are accurate within a factor of 2. First, we will review the basic LAP parameters (Sec. III.A).

A. Relationships Among Ablation Parameters: Ablation Efficiency

The momentum-coupling coefficient C_m is defined as the ratio of impulse density μv_E to the incident laser-pulse fluence Φ (or pressure p to intensity I for a CW laser), where exhaust velocity $v_E = \langle v_x \rangle$ is the first moment of the velocity distribution [39] $f(v_x)$ along the thrust axis x:

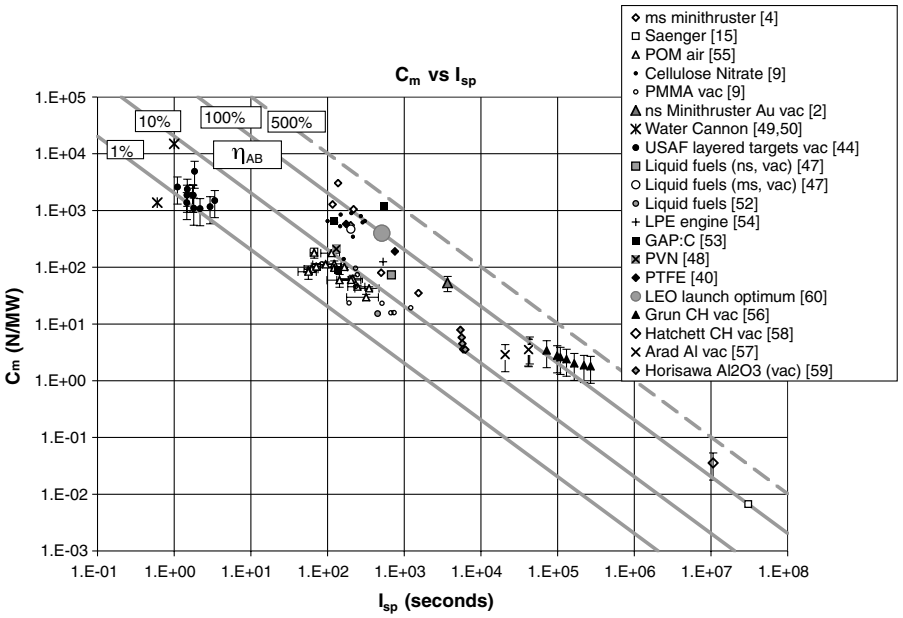

Fig. 6 Broad demonstrated operating range of laser-ablation propulsion, bounded on the right by the parameters of pure-photon propulsion (as a reference only). Typical data are shown. Numbers in the legend denote references. All data are in air, except as noted (vac denotes vacuum data). Ablation efficiency η_{ab} shown assumes $\psi = 1$. For photons, I_{sp} depends on the reference frame.

$$C_m = \mu v_E/\Phi = p/I \tag{2}$$

In Eq. (2), μ is the target areal mass density. Often, this distribution will be a drift Maxwellian of the form [39,60,61]

$$f(v_x, v_y, v_z) = C_x C_y C_z\{\exp -\beta[(v_x - u)^2 + v_y^2 + v_z^2]\} \tag{3}$$

with significant Mach number $M_s = u/c_s$. Defining specific ablation energy Q^* as the ratio

$$Q^* = \Phi/\mu \tag{4}$$

the relationship

$$v_E = C_m Q^* \tag{5}$$

offers a convenient way of determining exhaust velocity, since both C_m and Q^* are easily determined from impulse and mass-loss measurements. Specific impulse is related to exhaust velocity by

$$I_{sp} = v_E/g_o \tag{6}$$

and is a useful concept in rocketry, since it is also the impulse created by unit *weight* of fuel on the launch pad,

$$I_{sp} = Mv_E/(Mg_o) \tag{7}$$

with dimensions of N · s/N or seconds. Ablation efficiency

$$\eta_{ab} = \mu\psi v_E^2/(2\Phi) \tag{8}$$

is the efficiency with which laser-pulse energy density Φ is converted into exhaust kinetic-energy density $\mu\psi v_E^2/2$. It is related to the other parameters by

$$\eta_{ab} = \psi C_m v_E/2 \tag{9}$$

where [60]

$$\psi = \frac{\langle v_x^2\rangle}{(\langle v_x\rangle)^2} = \left\{\frac{u^2 + (kT/m_E)}{u^2}\right\} \tag{10}$$

Equation (9) can be restated to show that C_m and I_{sp} form a constant product controlled by the parameter η_{ab},

$$C_m I_{sp} = 2\eta_{ab}/(\psi g_o) \tag{11}$$

in a consistent unit system. We usually take $\psi = 1$ because it can be shown [39] that typical ablation plume shapes correspond to $\psi \le 1.15$. In any case, choosing $\psi = 1$ underestimates η_{ab}. For clarity, we will make this assumption from here on.

Note that a problem arises with Eqs. (4–8) when, as is often the case, an ablation measurement occurs in air, but only the ablated mass density μ is measured, ignoring the mass μ', which is added by reaction of the ablatant with air. As we will see in Sec. IV.C.2, this situation can easily lead to $\eta_{ab} > 1$, because Q^* in Eq. (4) and, subsequently, I_{sp} from Eq. (6) are overestimated. For this reason, we have not included any data from airbreathers in Fig. 6. A second cause for this condition is when the ablatant is exothermic, because the definition equation (8) addresses only optical, not chemical, energy input. When the chemical energy input is documented, we have included data of this sort in Fig. 6. This definition is deliberate and useful, because it relates directly to the electrical input power required to drive the laser that drives a device in space.

Note that if we use C_m in mixed units (dynes/watt), the 2 in Eq. (11) becomes 2E7. Equations (9) and (11) are useful as a reality check. If, for example, it is claimed that $C_m = 0.1$ N/W has been obtained in a particular situation, we should expect $I_{sp} \le 2.0$ s, even if $\eta_{ab} = 100\%$. It is impossible that $I_{sp} = 100$ s under the same conditions.

With laser repetition frequency f, laser average power $P = fW$, and the fuel consumption rate depends inversely on I_{sp}^2:

$$\dot{m} = \frac{P}{Q^*} = P\frac{2\eta_{ab}}{g_o^2 I_{sp}^2} \tag{12}$$

In the following three sections, we will review the theory that allows us to predict C_m in the fully formed plasma regime at lower intensities governed by vapor production and a new result that allows us to smoothly combine the regimes.

B. Momentum Coupling in the Plasma Regime

For laser intensities high enough to form a fully ionized plasma, the impulse delivered to a target by a laser pulse can be predicted with factor-of-2 accuracy using relationships that were adapted from inertial confinement fusion research [62]. In the plasma regime, absorption is via inverse bremsstrahlung (i.e., absorption due to inelastic scattering of photons by free electrons). The plasma becomes more dense until the critical density of electrons

$$n_{ec} = m_e n^2 \omega^2 / 4\pi e^2 = 1.115\text{E}27/\lambda_{\mu\text{m}}^2 \text{ m}^{-3} \quad (13)$$

is reached; beyond that, plasma absorption and reflection shields the target. The plasma frequency is

$$\omega_p = [4\pi n_e^2/m_e]^{1/2} \quad (14)$$

The optical absorption coefficient is

$$\alpha = \frac{2\omega}{c} k = \frac{\nu}{nc}\left[\frac{\omega_p^2}{\omega^2(1+\nu^2/\omega^2)}\right] \quad (15)$$

Using Eq. (13), $\omega_p^2/\omega^2 = n_e/n_{\text{ec}}$ and

$$\alpha = \frac{\nu}{nc}\left[\frac{n_e}{n_{\text{ec}}(1+\nu^2/\omega^2)}\right] \quad (16)$$

we have in the limits $\nu/\omega \ll 1$ and $n \approx 1$,

$$\alpha_{\text{IB}} \cong (\nu_{ei}/c)(n_e/n_{\text{ec}}) \quad (17)$$

and the laser-absorption depth in the plasma can be written as [62]

$$x_\alpha = \frac{1}{\alpha_{\text{IB}}} = \left(\frac{\nu_{ei}}{c}\frac{n_e}{n_{\text{ec}}}\right)^{-1} = \frac{2^{5/2} c A m_p k^{3/2} n_{\text{ec}} T_e^{3/2}}{\pi^{3/2}\sqrt{m_e} Z e^4 n_e^2 \ell_n \Lambda} = b\frac{n_{\text{ec}} T_e^{3/2}}{n_e^2} \quad (18)$$

decreasing proportionally to λ^2 because of the n_{ec} factor. This depth can be much smaller than the optical absorption depth in otherwise-transparent target materials, as small as a wavelength of the incident laser light, similar to the absorption depth in metals.

These conditions were used to develop simple expressions [62] for C_m on the target surface and for the I_{sp} generated in the plasma regime:

$$C_m = 1.84\text{E} - 4\frac{\Psi^{9/16}/A^{1/8}}{(I\lambda\sqrt{\tau})^{1/4}} \text{ N/W} \quad (19)$$

$$I_{\text{sp}} = 442\frac{A^{1/8}}{\Psi^{9/16}}(I\lambda\sqrt{\tau})^{1/4} \text{ s} \quad (20)$$

where A and $Z = n_e/n_i$ are, respectively, the mean atomic mass number and mean ionization state in the ablation plume. In turn, Z is determined by Saha's equation (see Sec. III.D). Please note that $\Psi = A/2[Z^2(Z+1)]^{1/3}$ in Eqs. (19) and (20) is not the same as ψ in Eq. (10). These relationships gave good predictions of plasma-regime experimental data on metals and C-H materials at multiple wavelengths and pulse durations from roughly 100 ps to 1 ms (Fig. 7).

C. Momentum Coupling in the Vapor Regime

The vapor regime is considerably more complex. At least four questions arise from applying the plasma-regime model:

1) What is the minimum pulse duration for which it applies? It is clear that the relationship equation (19) blows up at zero pulse width.

2) What is the lower limit of laser intensity for which it is valid? It is clear that the relationship equation (19) blows up at zero intensity.

3) What model applies to interactions below the plasma-initiation boundary?

4) How do we make a smooth transition between the models?

For the first question, Ihlemann et al. [63] showed experimentally that ablation ceases to obey our plasma model for laser pulses shorter than about 100 ps.

With regard to the second question, Fig. 8 gives an approximate relationship [64] for the onset of plasma formation based on a different selection of published data. The transition to the plasma regime is essentially complete an order of magnitude above intensities indicated in the figure. Since 1-D thermal transport theory [65] shows that surface temperature varies with time according to

$$T(t) = \frac{2I_o}{K}\left(\frac{\kappa\tau}{\pi}\right)^{1/2} \quad (21)$$

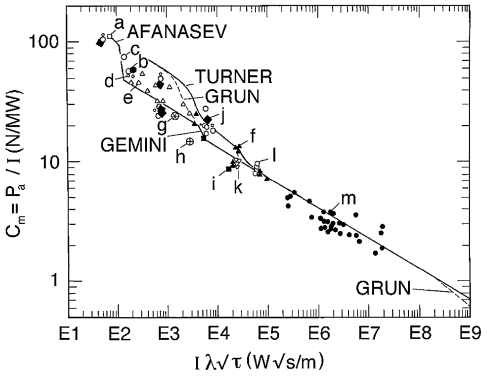

Fig. 7 Published data for impulse coupling coefficient on C-H materials are compared with the plasma-regime model [62]. Data are modeled in four subsets with distinct Saha equations governing ionization state. These are UV short pulses (Turner, 248 nm, 22 ns), midspectrum short pulses (Grun, 1.06 μm, 5 ns), midspectrum long pulses (Afanas'ev, 1.06 μm, 1.5 ms), and infrared long pulses (Gemini, 10.6 μm and 1.8 μs). These names and the data labels are explained in [62]; used with permission from the American Institute of Physics, copyright 1988.

In Eq. (21), K is the thermal conductivity and κ is the thermal diffusivity of a solid material. It should not come as a surprise that the intensity required to reach the plasma-ignition temperature on a surface varies in such a way that $I\tau^{1/2}$ is constant, as shown in Fig. 8 (above 100 ps).

The vapor regime (third question above) is conceptually far more complex. The target material may be in vacuum or in air. In the latter case, Root [66] has defined three subdivisions of the laser–target interaction, which are summarized in Table 2. These are laser-supported combustion (LSC), laser-supported detonation (LSD), and laser-supported rarefaction (LSR). Figure 9 shows the range of pressures observed in the vapor regime [66].

How significant is the tamping effect of ambient air on laser-produced vapor pressure? Pirri [67] gives a discussion of this phenomenon.

The velocity of the LSD wave is given by [68]

$$v_D = \left[\frac{2(\gamma^2-1)I}{\rho_o}\right]^{1/3} \quad (22)$$

from which the pressure

$$p_D = \frac{\rho_o v_D^2}{(\gamma+1)} \quad (23)$$

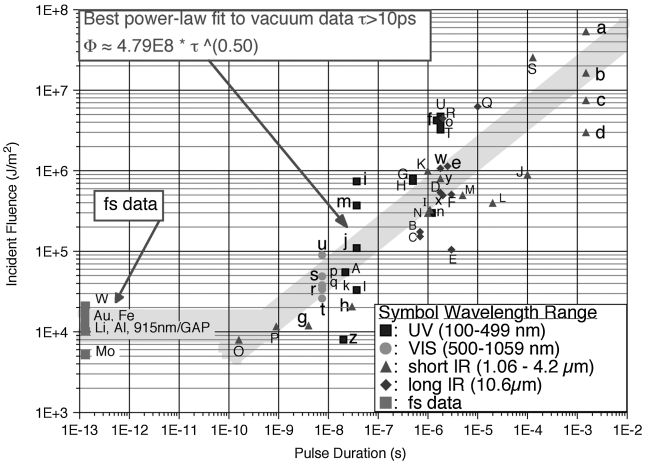

Fig. 8 Fluence required for plasma ignition on targets in vacuum across the entire range from 100 fs to 1 ms. 1-D thermal diffusion theory governs the range 100 ps $< \tau <$ 1 ms. $\Phi = F\tau^{0.5}$ corresponds to $I = F/\tau^{0.5}$. This plot shows that it takes less pulse energy to make a plasma as τ gets shorter, down to about 100 ps. Data labels are explained in [64].

Table 2 Vapor-regime subdivisions after root

Parameter	LSC	LSD	LSR (transition to plasma regime)
Absorption zone (temperature is highest here)	Located in the partly ionized vapor adjacent to target, behind a weak shock forming in ambient gas	Moves to the shock that forms above the target as the shock becomes stronger	Initiated at speed of light by hot-target plasma radiation; begins in the ambient gas relatively far from the target, propagates toward the target
Mechanism causing transport	Radiative transfer from the hot plasma to the cool high-pressure gas created in the shock wave	Fluid dynamics of shock propagation	Radiative transfer from the hot plasma to ambient gas
Temperature	0.1 to a few electron volts	A few to tens of electron volts	Above tens of electron volts
Laser intensity	Low	Intermediate	Up to plasma threshold

After expansion of the gas behind the detonation, the surface-pressure contribution is

$$p_{s1D} = \left[\frac{(\gamma+1)}{2\gamma}\right]^{[2\gamma/(\gamma-1)]} \tag{24}$$

In Eqs. (23) and (24) , ρ_o is vapor mass density and $\gamma = C_p/C_v$ is the ratio of the constant-pressure and constant-volume specific heats. If we define a ratio

$$\mathcal{M} = \frac{p + p_{s1D}}{p} \tag{25}$$

(Fig. 10), we conclude that tamping is a 20–50% effect for the intensity range shown in the figure and need not be considered for estimating surface pressure to within a factor of 2. When surface plasma is formed in ambient air, the pressures are larger yet, and Eq. (25) shows that $\mathcal{M} \Rightarrow 1$. For example, in other measurements [69], with $I = 1.4$ TW/m^2 at $\lambda = 10.6$ μm on aluminum, the experimental pressure increase was even less than that predicted by Pirri [67] when going from vacuum to ambient atmosphere.

Given all this conceptual complexity, it is stunning that the log-pressure-vs-log-irradiance plot for typical targets (Fig. 9) closely follows a simpler power law for the LSC and LSD regimes. That fact and Fig. 10 suggest that a simple model that incorporates both vapor and plasma physics might fit this data to within an rms deviation factor of 2.0 without considering the detailed physics of the interaction with ambient air.

The approach to be used in modeling depends entirely on the data that are available for the target material. If we know just the threshold fluence Φ_o, solid density ρ_s, and laser-absorption coefficient α in the ablation zone, new work by Sinko and Phipps [70] has provided an elegant model that meets our accuracy requirement in modeling impulse in the vapor regime. On the other hand, if a vapor-pressure table (p vs T) exists for the material at pressures up to tens of kilobars and temperatures up to the vicinity of 1E6 K, then a numerical approach [71] gives good results and represents one additional level of complexity in modeling the material.

In the Sinko model, beginning with the Beer–Lambert–Bouger absorption law [72], we can write [73] for the etch depth,

$$x_v = (1/\alpha)\,\ell n(T\Phi/\Phi_o) \tag{26}$$

and

$$\mu = (\rho_s/\alpha)\,\ell n(T\Phi/\Phi_o) \quad \text{g/cm}^2 \tag{27}$$

for the ablated mass areal density. The momentum areal density σ is then tied to the laser parameters by energy conservation (T is transmissivity to the ablation region):

$$\sigma^2/2\mu = T\Phi - \Phi_o \tag{28}$$

whence

$$C_m = \frac{\sigma}{\Phi} = \sqrt{\frac{2\mu(T\xi-1)}{\Phi_o\xi^2}} = \sqrt{\frac{2(\rho/\alpha)\,\ell n\,\xi(T\xi-1)}{\Phi_o\xi^2}} \tag{29}$$

and

$$I_{\rm sp} = \frac{\Phi C_m}{\mu g_o} = \sqrt{\frac{2\Phi_o(T\xi-1)}{g_o^2(\rho/\alpha)\,\ell n\,\xi}} \tag{30}$$

where $\xi = \Phi/\Phi_o$, with an ablation efficiency given by

$$\eta_{\rm ab} = (g_o/2)C_m I_{\rm sp} = T - 1/\xi \tag{31}$$

Equation (31) implies that $\eta_{\rm ab} \Rightarrow T$ in the large fluence limit, as it should, that $\eta_{\rm ab} \Rightarrow 0$ when $\Phi/\Phi_o = 1/T$ and, e.g., $\Phi/\Phi_o = 2$ if $T = 0.5$, which also makes sense.

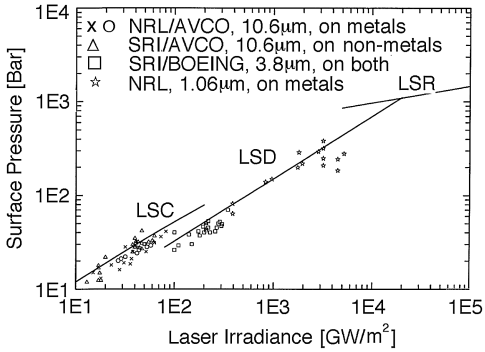

Fig. 9 Pressure vs laser irradiance on the target for experiments in which the three types of absorption waves were induced. Data source abbreviations are NRL: U.S. Navy Research Laboratory; AVCO: Avco Corporation, now a subsidiary of Textron Systems Corporation; SRI: Stanford Research Institute; and BOEING: The Boeing Company Research Laboratory. Laser wavelengths ranged from 1.06 to 10.6 μm. Note that a typical coupling coefficient $C_m = p/I = 100$ N/MW is represented when a pressure of 10 bar (1E6 N/m^2) is developed by an irradiance of 10 GW/m^2. Figure is based on [66] and used with permission from the rightsholder.

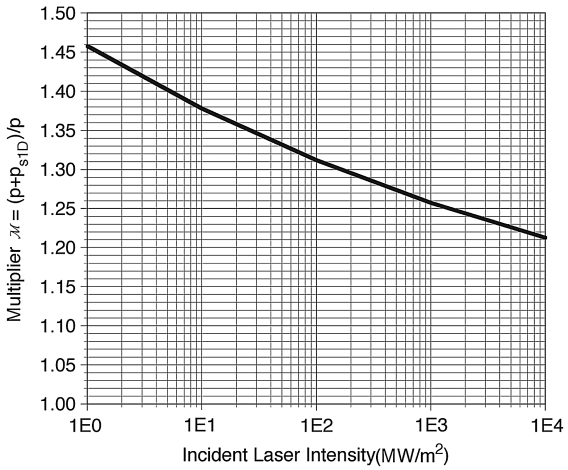

Fig. 10 Pirri multiplier is not significant within the factor-of-2 accuracy we have set for this review and for intensities in the vapor regime.

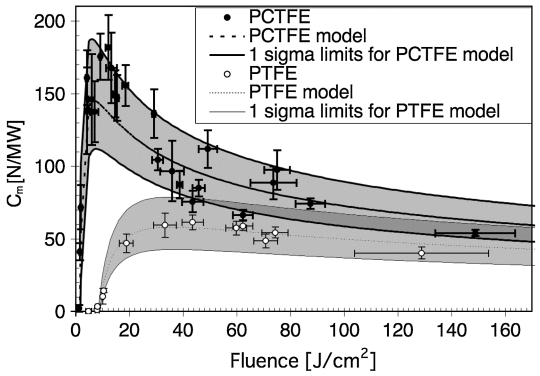

Fig. 11 The Sinko model predicts C_m for pulsed CO_2-laser radiation C_m on polychlorotrifluoroethylene polymer (PCTFE) below and perhaps slightly into the plasma regime. PTFE denotes polytetrafluoroethylene (Teflon). Modeling limits ($\pm 1\sigma$ parameter estimates) and experimental error bars ($\pm 1\sigma$) are included. Each point is an average of 5–10 shots (see [70]); used with permission from the American Institute of Physics, copyright 2009.

Figure 11 demonstrates the success of the Sinko model [70].

D. Connecting the Two Regimes

The Saha equation [74]

$$\frac{n_e n_j}{n_{j-1}} = \frac{2u_j}{u_{j-1}}\left(\frac{2\pi m_e kT_e}{h^2}\right)^{3/2} \exp(-W_{j,j-1}/kT_e) \tag{32}$$

gives the relative densities of the jth and $(j-1)$th ionization states. In Eq. (32), the u_j are the quantum mechanical weighting functions for the jth state. For example, for Al, $u_1 = 1$ and $u_o = 6$. We will consider only intensities sufficient to make $Z = 1$ in this paper, and in this case, a simple expression for the ionization fraction η_i can be obtained:

$$\eta_i = n_i/(n_o + n_i) \tag{33}$$

where η_i and n_o are the ion and neutral number densities. We consider the vapor and plasma in the region adjacent to the target surface to be isothermal. Then

$$p = (n_o + n_e + n_i)kT \tag{34}$$

so that $n_o + n_e + n_i = n_o + 2n_e$ is limited by

$$n_o + 2n_e = \frac{p}{kT} \tag{35}$$

(since $n_i + n_e = 2n_e$ for single-stage ionization). Then, where

$$B_{\text{Saha}} = \frac{2u_1}{u_o}\left(\frac{2\pi m_e kT}{h^2}\right)^{3/2} \tag{36}$$

we obtain

$$n_e = \sqrt{n_o B_{\text{Saha}}}\exp(-W_{1,0}/kT) \tag{37}$$

and an ionization fraction:

$$\eta_i = 2n_e/(n_o + 2n_e) \tag{38}$$

Equation (38) provides the mechanism for connecting the two models smoothly. Denoting C_{mp} and C_{mv} as the momentum-coupling coefficients given by Eqs. (19) and (29), respectively, we just use the ionization fraction given by Eq. (38) to adjust the relative weights of the contributions from the vapor and plasma models:

$$C_m = [\eta_i p_p + (1-\eta_i)p_v]/I = \eta_i C_{mp} + (1-\eta_i)C_{mv} \tag{39}$$

Figure 12 [55–57,62,75,76] shows the success of this approach, for the first time providing a relatively straightforward expression for calculating momentum-coupling coefficients over the entire intensity range from ablation onset through the plasma regime for a given material and given laser parameters. In the figure, the abscissa variable is $I\lambda\tau^{1/2}$, which is a necessary choice to show the transition to materials in the plasma regime in which this is the appropriate scaling parameter. This choice also tends to aggregate C_{mv} data taken for the same wavelength and material, because their vaporization thresholds will scale like $I\tau^{1/2}$.

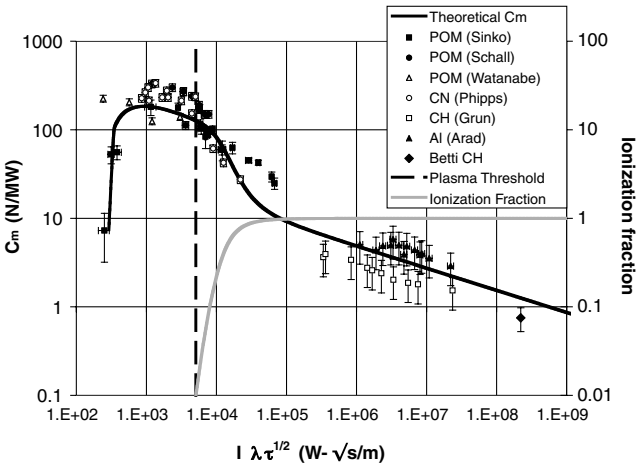

Fig. 12 Equation (40) model fits data reasonably well from ablation threshold up to inertial confinement fusion conditions. Data: POM (Sinko and Pakhomov [55]), POM (Schall [75]), POM (Watanabe [76]), cellulose nitrate (Phipps et al. [62]), CH (Grun et al. [56]) , Al (Arad [57]) and Betti CH (private communication with R. Betti, 2008). Dashed line: plasma threshold; solid black line: Eq. (40) model; and solid gray line: ionization fraction.

Finally, maximizing Eq. (29) gives an optimum fluence for achieving maximum C_m in the Sinko model, which should also apply to the connected model, because entering the plasma regime can only reduce coupling. This optimum is given by

$$F_{\text{opt}} = 4.244\Phi_o \text{ J/m}^2 \tag{40}$$

The threshold Φ_o is determined experimentally.

IV. Propellants

A. Designing Optimum Polymer Propellants

The first version of the laser–plasma thruster (discussed in Sec. V.A) required specially designed ablatants (laser-ablation propellants) that exceeded the capabilities of common commercial polymers. The key requirements were very low thermal conductivity (because of the millisecond-duration laser pulses employed in that device) and maximum exothermic energy content, to give maximum thrust-to-power ratio.

Various commercially available and specially designed polymers were tested [77–82]. Three different polymers [glycidyl azide polymer (GAP), polyvinyl nitrate (PVN), and polyvinyl chloride (PVC), with structures shown in Fig. 13] with two different absorbers [carbon nanoparticles and an infrared (IR) dye (Epolite® 2057)] were studied as fuel for the laser–plasma thruster.

GAP and PVN are energetic polymers with a high decomposition enthalpy of -3829 J/g (PVN) and -2053 J/g (GAP). PVC was used as a less-energetic commercially available reference material (the decomposition enthalpy of -418 J/g is much lower than for the other two polymers).

To evaluate the performance of the polymers, experiments were performed [83–85] at low fluence with shadowgraphy in air and at high fluence with thrust measurements in vacuum, plasma emission spectroscopy in air and vacuum, and mass spectrometry in vacuum. Different laser-pulse lengths ranging from femtoseconds to microseconds were also applied. The shadowgraphy measurements were performed with nanosecond laser pulses at fluences below the plasma threshold fluence. The main advantage of this method is the relatively simple setup, as the experiments were performed in air. The main

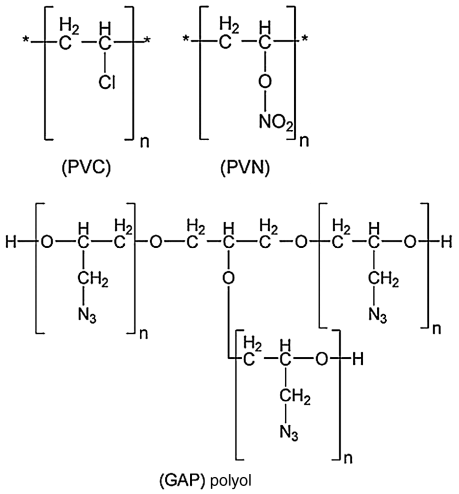

Fig. 13 Chemical structures of the studied polymers.

features that can be observed are the propagation of the shock wave and the composition and propagation of the particle plume. Measured shock wave velocity was in good agreement with the energetic properties of the polymers. The fastest shock wave was observed for PVN + C, followed by GAP with both absorbers and PVC + C. For all carbon-doped polymers, large amounts of solid- or liquid-polymer fragments were visible in the ablation plume, whereas in the case of GAP + IR, no large fragments were visible (shown in Fig. 14). This indicates a higher degree of fragmentation for GAP + IR and therefore a high release of chemically stored energy. For PVN + IR, strong thermal features were observed: i.e., the formation of fibers and melting. Plasma emission spectroscopy in air facilitated calculation of electron density and plasma temperature from specific emission lines (Balmer H_α and CN violet), yielding values of $\sim$1E24 m^{-3} for the electron density and 7500 K for the plasma temperature.

The vacuum plasma emission and the mass spectrometry experiments at high laser fluences ($\sim$25 J $\cdot$ cm^{-2}) revealed that the highest velocities were observed for C^+ species. A higher degree of fragmentation was observed for the energetic polymers with the mass spectrometer after nanosecond-pulse irradiation. In the mass spectra of PVC + C and PVN + C, strong signals could be assigned to the solvent that was used to solvent-cast the polymers. This trapped solvent acts as inert material during the ablation process and can therefore have a negative influence on the thrust properties of the two polymers. The influence of the pulse length was investigated with plasma emission spectroscopy measurements. They were performed with femtosecond and nanosecond laser pulses in vacuum. In femtosecond experiments, three domains with different velocities could be observed. The domain with the highest propagation velocity was formed by ionized species that were accelerated by a coulomb explosion on the sample surface. A second domain could be assigned to neutral atoms. The third domain was formed by diatomic species. A fourth domain consisting of nanoparticles was observed with plasma imaging. These nanoparticles were only observed for the polymers with carbon nanoparticles as absorbers. The investigated species generally moved faster for femtosecond irradiation than for nanosecond irradiation. The influence of the polymer on the expansion velocity was less pronounced for femtosecond irradiation, for which similar expansion velocities were determined for all polymers, suggesting that almost all materials can be used in a laser–plasma thruster (LPT) with a femtosecond laser as the laser source and that the achievable thrust may also be higher.

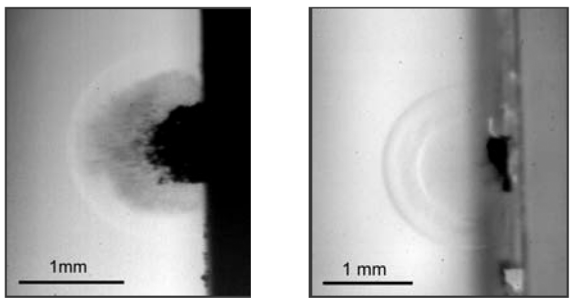

a) b)

Fig. 14 Shadowgraphy images taken 1 μs after irradiation at 1064 nm: a) GAP + C and b) GAP + IR.

The highest thrust values for millisecond laser irradiation were obtained for GAP + C, followed by GAP + IR. For both polymer-absorber systems, maximum efficiencies of over 100% (370% for GAP + C and 200% for GAP + IR) and a specific impulse of 860 s for GAP + C were measured [86]. For PVC + C, an efficiency of 50% was obtained. The lowest efficiency values were measured for PVN + C, with only 21%. This low value for the most energetic polymer is probably caused by trapped solvent in the film and by thermal effects observed for this polymer (melting and splashing), resulting in a waste of energy from the laser and material. Thrust probably originates from a combination of volume explosion from the polymer decomposition, coulomb repulsion, and impulse from larger, fast-traveling, fragments. Thrust measurements showed that the LPT is, in reality, a hybrid thruster, for which chemical stored energy from the fuel polymer and laser energy together produce high thrust values. An important factor seems to be exothermic decomposition, but other material properties have a strong influence on the resulting thrust. PVN decomposes very energetically, but showed the worst performance in thrust measurements. The strong thermal effects and trapped solvent in the PVN films are probably responsible.

B. Liquid Propellants

The main disadvantage of solid fuels in millinewton-thrust engines is the use of a tape as fuel dispenser (see Sec. V.A), which adds extra mass to the satellite and also induces undesirable angular momentum due to the rotation of reels. The alternative is to use liquid fuels, stored in a tank, with good energy density and to dispense according to need. Obviously, the propellant must have a viscosity low enough to allow it to be pumped through a nozzle. On the other hand, previous work has shown that the ablation of liquid targets yields very low specific impulse [87]: for instance, 19 s with carbon-ink-doped water [88]. This is essentially due to the splashing of the liquid, which uses the laser energy for droplet formation instead of high-velocity plasma acceleration. Moreover, splashing materials would contaminate the laser optics and satellite surfaces, compromise the reliability of the system, and energy stored in the energetic fuel would also be lost. Therefore, it is essential to find appropriate conditions under which the liquid fuel does not splash.

One way to eliminate splashing is to increase the viscosity of the liquid fuel. Four liquid solutions of GAP were analyzed by shadowgraphy to test if liquid-polymer solutions are applicable or even superior to solid fuels in laser–plasma thrusters. At low fluence, all concentrations had the same behavior and no liquid is ejected at 10 μs. As fluence increased, the less viscous solutions first produced splashing: first the 28% solution, then the 50% solution. The 70% GAP sample avoided splashing behavior at the highest applied fluence ($\sim$7 J $\cdot$ cm^{-2}) at which plasma onset was observed. Shadowgraphy images revealing the splashing for the lower concentrations and nonsplashing for the highest concentration are shown in Fig. 15. This shows that suitable conditions can be found for using a liquid-GAP solution as fuel for LPTs. The splashing behavior is controlled by the viscosity of the solution and the applied laser fluence [89,90]. The specific impulse of the 70% GAP + IR solution was measured to be 680 s (see Sec. V.A), which is even higher than the 250 s obtained for solid GAP doped with infrared dye [91].

A second approach to mitigating splashing is in novel propellant geometries such as thin films or one-dimensional streams [92] or even pointlike droplets [93,94] to minimize liquid-ejection losses.

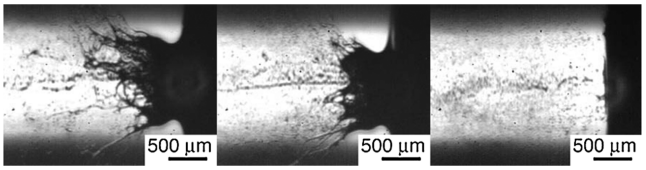

Fig. 15 Pictures taken after 10 μs with 4.5 J/cm^2 for varying GAP concentrations (left to right: 28, 50, and 70%); adapted from a more complete data set in [90].

The geometry of the surface of the liquid, within the same container, can make a significant difference [94] (Fig. 16) [95].

Laser ablation of bulk liquids for propulsion was thoroughly investigated by Aoki et al. [87] and by Sinko and Pakhomov [92]. Results conclusively show that C_m is enhanced, but I_{sp} is impaired with these propellants (Fig. 17) [96,97].

For materials with large α, ablation occurs at the liquid surface (surface ablation), forming a vapor plume, but for materials with low α, ablation centers also form within the liquid itself (volume ablation), as shown in Fig. 18 [95], 10 μs after arrival of the transversely excited atmospheric (TEA) CO_2 laser pulse. At higher irradiances, plumes form above the surface, even for ablation of low-α liquids.

By using thin-liquid films, splashing losses can be minimized and the area of interaction can be maximized. Yamaguchi et al. [94] showed that the best results are obtained with a transparent film of propellant liquid overlying an absorbing substrate. The convention has been to term such systems *cannons*, since dense material is ejected by expanding gases, as in a cannon. Ablation of thin films can be categorized based on the absorption properties of the propellant and substrate. Measurements [46] with an absorbing substrate and a transparent liquid-propellant layer achieved significant I_{sp}, calculated using both the total liquid volume and mass removal from the substrate.

Results are shown in Fig. 19 for water, ethanol, and hexane films (all approximately 75 μm thick) atop a Delrin (POM) substrate, compared with the results for the bulk fluids. Other authors' measurements for the water cannon [49], acrylic cannon [94], and glycerin droplets [93] are included for comparison. It is noteworthy that about a two-order-of-magnitude improvement in ablation efficiency relative to bulk liquids is obtained in thin films of transparent liquid over a POM absorber. Table 3 compares the approaches.

Figure 20 [96] allows comparison of the portions contributed to C_m by the POM substrate and by the liquid films.

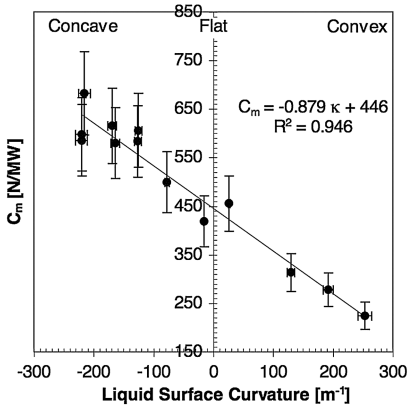

Fig. 16 Effect of surface curvature on C_m for 0.4 J/pulse CO_2-laser ablation of water (see [95]); used with permission of the American Institute of Physics, copyright 2006.

C. Effect of Nozzles on C_m and I_{sp}

1. *DLR Experiments*

In the DLR work [98,99], a parabolic reflector was employed both as a focusing component and as a nozzle, with both atmospheric air and POM at the reflector focus. The CO_2 laser generated 10 ms, 10.6 μm pulses at 100 Hz maximum [100]. The geometry employed was called the Bohn bell [101] (Fig. 21).

An LSD wave was created at the thruster focus above the 100 GW/m^2 breakdown threshold in a 4-mm-radius focal spot at 100 J pulse energy [102]. A photodetector showed that 14 μs after an initial peak, a second, stronger, recombination light peak was seen that resulted from reheating of the gas by the shock wave reflected at the apex. Two corresponding shock waves were found exiting the thruster.

Calculations showed that exhaust velocity and pressure were higher behind the second shock front. Modeling using Sedov theory [103] included the detailed laser-pulse shape (a high energy spike and a sawtooth-shaped tail), the shock wave reflected inside the thruster, with the temporal development of the pressure distribution acting on the thruster wall and the propagation of the expanding gas. Experimental results indicated supersonic exhaust velocities. The measured coupling coefficients were about one order of magnitude lower than the values from the integration of the modeled pressure distribution, probably because of effects such as radiation losses, heat conduction, and deformation, which were not modeled. Also, Sedov theory may not be applicable in the later course of gas expansion.

First, the effect of the nozzle shape on C_m without a solid propellant was studied. According to Ageev et al. [104], an increasing inlet angle ϑ results in a decrease of C_m, leading to an optimum nozzle length. This effect was confirmed in a comparative study by Myrabo et al. [101]. C_m also slightly increased with length in parabolic nozzles with lengths of 6, 12, and 18 cm [105]. For the baseline thruster, C_m was enhanced by 50% by adding a 7.7-cm-diam, 16.5-cm-long tube to the thruster aperture, effectively reducing ϑ from 87 to 22° A similar effect was observed when launching the thruster in a free-flight experiment [106].

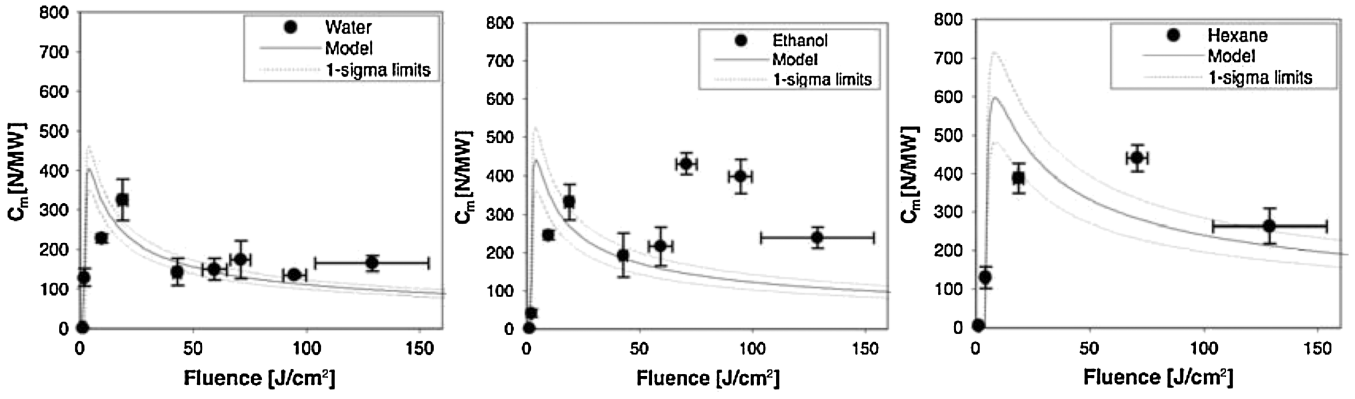

Fig. 17 Coupling coefficients obtained for water (left), ethanol (center), and hexane (right) (see [95]); used with permission of the American Institute of Physics, copyright 2006.

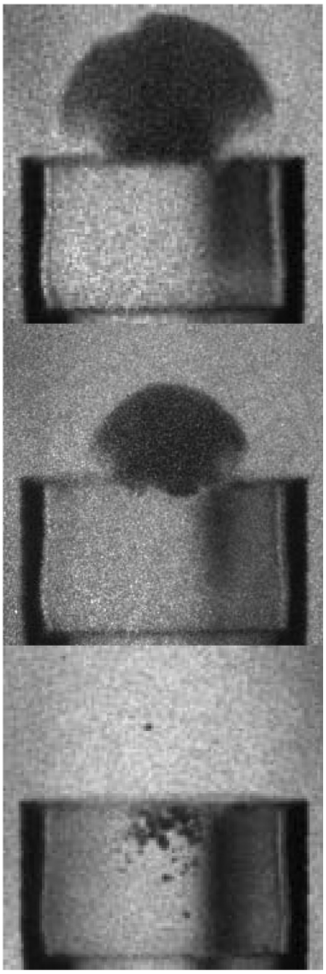

Fig. 18 Ablation of water (top) ethanol (center) and hexane (bottom) for 0.4 J/pulse and 5 mm^2 spot area at 10 μs, using CO_2-laser radiation (see [95]); used with permission of the American Institute of Physics, copyright 2006.

For these tests, the inlet diameter was chosen to match the laser system beam diameter. However, calculations based on Sedov theory showed that optimum coupling would be achieved if the thruster were shrunk by a factor of 2, to fit the dynamic radius of the detonation at 100 J pulse energy at 1 atm. This change would require an external focusing unit.

Measurements in vacuum [107] gave data needed for mission analysis of a ground-based launch into orbit by laser propulsion. Analysis of momentum coupling vs ambient pressure surprisingly showed that C_m is not significantly affected by pressure down to 250 hPa [108]. This result enables ascent of a thruster using the ambient air as the propellant up to 11 km altitude and, with decreasing performance, up to 25 km altitude. Above that limit, a solid propellant would be required. Although the airbreathing mode can be combined with ablative propellants in the lower atmosphere, propulsion by laser-induced air breakdown may only be preferable for drag reduction and propellant economy [109].

A POM rod was then added to the parabola focus, positioned so that it could be illuminated either on the end surface or on an annular focus area of 8 mm diameter. Effects of the orientation of the ablator surface to the flight direction were studied [105]. Experiments in vacuum showed jet velocities of around 2.5 km/s for either configuration, but C_m was doubled for annular illumination [42]. The thruster's parabolic shape enhanced propulsion efficiency, both by nozzle effects and due to the absorption wave arising from the radial expansion of the POM vapor [106,110]. With the annular focus configuration, momentum coupling was enhanced by increasing the diameter of the POM rod and thus the amount of ablated mass. Optimizing C_m can also be achieved by varying pulse energies,

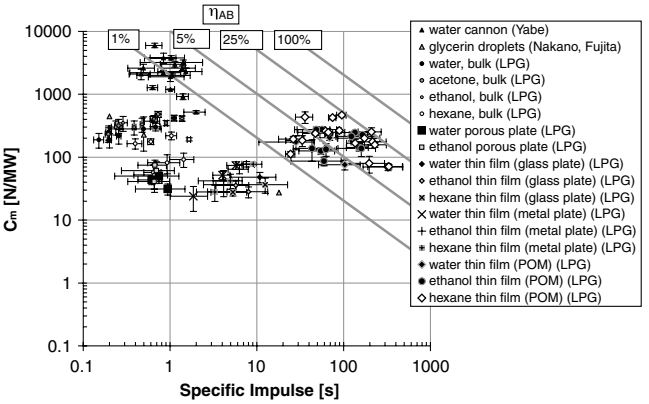

Fig. 19 C_m vs I_{sp} for thin films (typically 75 μm thick) of water ethanol and *n*-hexane atop Delrin substrate, and for the bulk fluids. References: Yabe et al. [49] and Nakano, et al. [93]. LPG refers to data taken by the Laser Propulsion Group at the University of Alabama at Huntsville.

keeping the enthalpy of the ablated propellant constant, or by tilting the ablation surface of a planar target [111].

Relative to vacuum ambient, results showed that for ablation of POM in ambient air, C_m is more than doubled (Fig. 22). Comparative measurements in N_2 atmosphere showed that combustion effects also add to the momentum coupling.

Flight experiments were conducted with the parabolic reflector. These had a short flight range, limited by the height of the laboratory ceiling, or were wire-guided [102] to keep the lightcraft aligned with the laser beam. To improve ignition reproducibility in these tests, a metal ignition pin was added at the reflector focus. A free-flight altitude of around 8 m was achieved [106] with 20 laser pulses of 150 J and 50 Hz.

A dynamic analysis of pulsed flights with respect to laser parameters with POM propellant in vacuum was performed [112]. Steering was investigated by tilting the ignition pin or the ablation rod inside the thruster [113]. In this way, lateral and angular impulse components were successfully induced to simulate the requirements of steering and stabilizing a laser-driven rocket during flight.

2. *University of Alabama at Huntsville Nozzle Studies*

To better understand the effect of nozzles on C_m and I_{sp}, data were taken on bare ablative propellant with 10.6 μm laser pulses with 300 ns duration and compared with data for the same propellant at the throat of diverging nozzles with area expansion ratios varying from 4:1 to 16:1 (Fig. 23) [114]. Because the experiments were done in air, several cases of $\eta_{ab} > 1$ are shown. Figure 24 shows an ablation experiment in operation.

Since POM is not exothermic, these are distortions of the actual I_{sp} due at least in part to the effect of propellant combustion in air adding unmeasured mass μ' to the measured propellant mass loss μ, an effect described in Sec. IV.A. For the Fig. 23 data, this may not be the only cause of the discrepancy in I_{sp}, since complete combustion of $(CH_2O)_n$ would affect I_{sp} by, at most, a factor of 2. The data is very valuable for showing the enhancement of C_m by using nozzles, which could potentially be realized for planar ablators such as the laser–plasma thrusters discussed in Sec. V.A.

D. CHO-Type Propellants

Laser ablation of solid CHO-chemistry materials is accompanied by both evaporation and thermal decomposition of the materials (pyrolysis) [115]. There are two pathways for this pyrolysis.

Table 3 Comparing methods of achieving good I_{sp} in liquids

Approach	Target material	I_{sp} obtained, s
Increased viscosity	GAP	680 (see Sec. V.A)
Liquid films	Hexane on POM	370
	Ethanol on porous plate	170

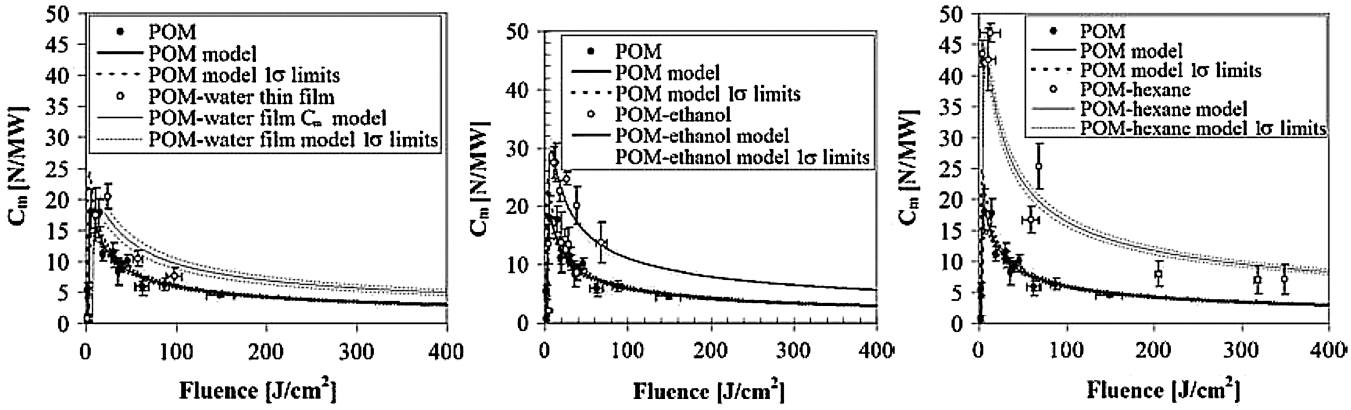

Fig. 20 Plots of C_m vs fluence for films of water (left), ethanol (center), and *n*-hexane (right) atop Delrin substrate and for the bare POM substrate with no film (all) (see [96]).

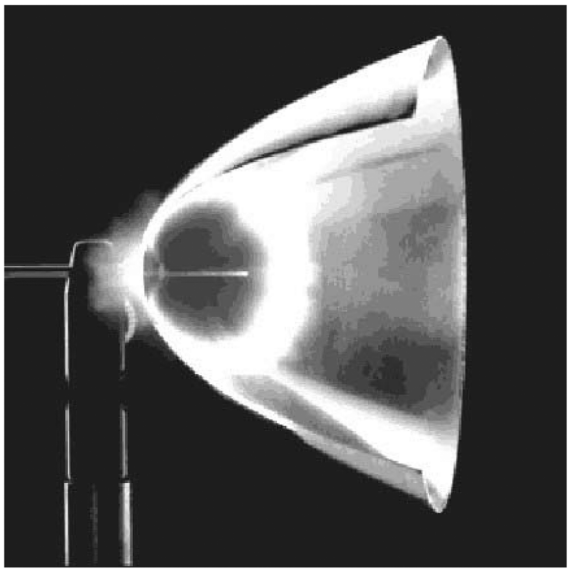

Fig. 21 Bohn-bell parabolic reflector. Ambient air is dynamically refreshed from the nozzle exit between pulses.

First is detonation of evaporated material, when a chemical oxidation reaction of the flammable components of the propellant propagates through a reaction region with a velocity exceeding a sound speed [116]. In this process, detonation energy Q_{det} is released and a high-power detonation wave is generated. Products of the decomposition of CHO-chemical propellants are carbon dioxide, water vapor, oxygen, and hydrogen (CO_2-H_2O-O_2-H_2).

Second is a delayed burning of the products in atmospheric air, which are not completely oxidized by the detonation, through which burning energy Q_{db} is released. The detonation and burning energies can be determined by Hess's law [117]:

$$Q_{\text{det}} = -(\Delta H_{\text{pr}} - \Delta H^{o}_{f298}) \tag{41}$$

$$Q_{\text{db}} = -\Delta H_{\text{pr}} \tag{42}$$

Ageichik et al. [118] studied laser radiation interaction with planar solid CHO-chemistry propellants, surface-absorbing target materials, and incident laser intensity chosen for maximum I_{sp}. The most important one of these is POM $(CH_2O)_n$, which plays a major role in developments discussed in Secs. IV.C.2, V.B, V.D, and V.E.

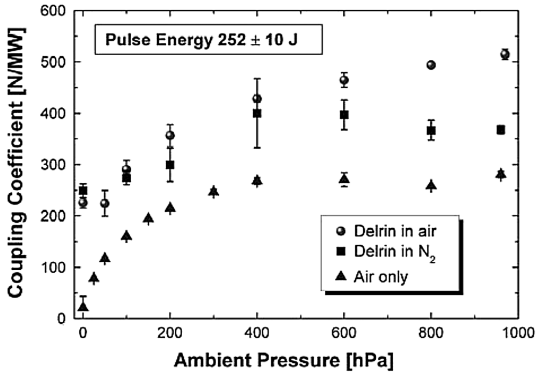

Fig. 22 Coupling coefficient for the parabola vs ambient pressure for different conditions.

V. State-of-the-Art Devices

A. Laser–Plasma Thrusters

Throughout the early history of extra-atmospheric propulsion, emphasis was on producing engines with ever-larger thrust, culminating with the 6800 kN Rocketdyne F-1 engines for Apollo and engines developed for the Energiya program. Now, with the advent of micro- ($\geq$ 10 kg), nano- (1–10 kg), and even picosatellites (less than 1 kg), this trend is reversing. For many applications, such as pointing and positioning spacecraft, a thrust on the order of 1 mN is desirable, together with low thrust noise and very small minimum-impulse bits. This is difficult to do with conventional chemical rockets.

To meet this challenge, LPTs were developed. LPTs have the advantages of programmable thrust, a minimum-impulse bit that may be as small as nano newton seconds, and elimination of the need for storing dangerous chemically reactive propellants on a spacecraft. Other advantages are thrust density, power-to-mass ratio on the order

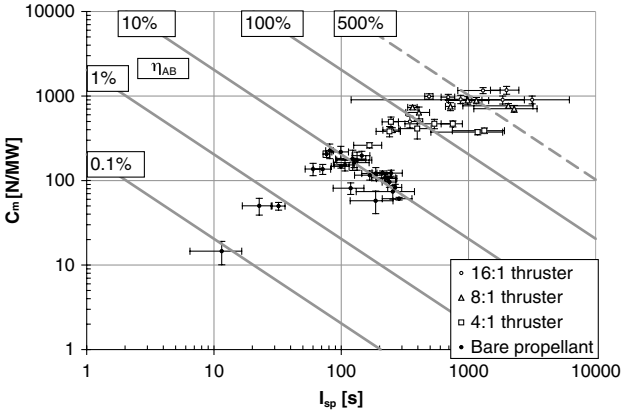

Fig. 23 Dramatic enhancement of ablation efficiencies by using nozzles of various expansion ratios with the POM ablatant is shown (see [114] for related work).

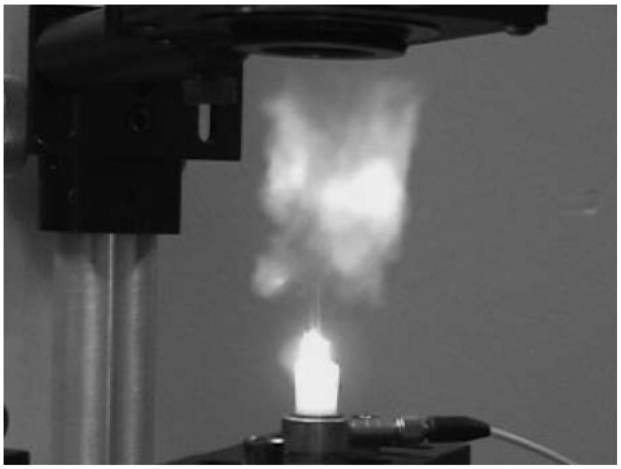

Fig. 24 Ablation experiment in operation.

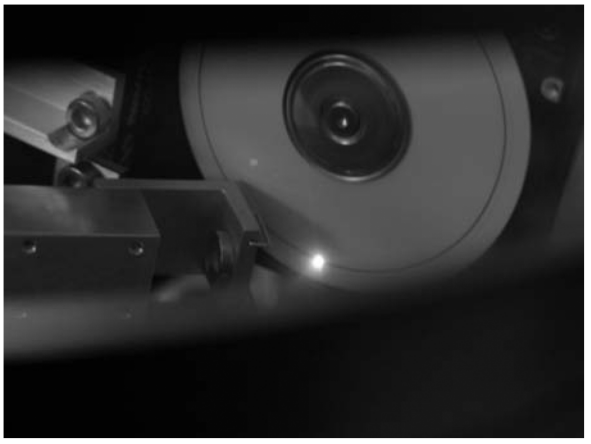

Fig. 26 The ns-LPT prototype during vacuum chamber tests (see [119]).

of 300 W/kg, and thrust efficiency greater than 100%, due to the energetic ablatant used.

Applications of LPTs are to spacecraft positioning and pointing in their present state of development. However, with liquid fuels, the design is extensible to units developing 6 N thrust in millisecond-pulse mode for agile spacecraft propulsion (see Sec. VI.A). By varying laser intensity, such a device could span the range of $120 < I_{sp} < 3660$ s almost instantly.

Two LPTs were developed, occupying opposite ends of the I_{sp} spectrum: the millisecond LPT (ms-LPT) [4,34] (Fig. 25) was designed for high thrust and, consequently, low I_{sp}, whereas the nanosecond LPT (ns-LPT) was intended for high I_{sp} and, consequently, low thrust. The ns-LPT research prototype [119] (Fig. 26) is competitive with ion thrusters for some applications.

High-power, single-facet, 920 nm diode lasers were used in the ms-LPT for brightness, low cost, and durability. A slit-focus illumination pattern on the target was chosen for the best overall target fill factor (Fig. 27). Bare-facet rather than fiber-coupled diodes were chosen for optical efficiency and brightness preservation.

For the ms-LPT operating at $\tau = 2$ ms, no metals or metal oxides (and only some polymers) have sufficiently low thermal conductivity and specific heat to reach the plasma threshold with the intensity that can be transmitted through a transparent polymer layer; even pure graphite did not meet these requirements. Ultimately, GAP was used as the ablatant; nanopearl carbon (typically 1–2% by mass) or infrared dyes were used as the laser absorber (see Sec. IV.A). A momentum-coupling coefficient $C_m = 3$ kN/MW was obtained (Table 4) for operating times of hours [4].

For the ns-LPT operating well into the plasma regime at $\tau = 4$ ns, any ablator material could be used, in principle. Phipps et al. [2] demonstrated $I_{sp} = 3660$ s with gold ablatant as well as 680 s on a viscous-liquid-GAP target (Sec. V.A). Table 4 summarizes results obtained with both devices.

Liquid-fuel test results [120] are summarized in Table 5. These results were obtained with GAP, partially polymerized to reach a viscosity of 200 Pa · s (see Sec. IV.B).

B. Laser-Driven In-Tube Accelerator

In-tube propulsion is a method to enhance propulsion performance by using the confinement of propellant in a launch tube so that the pressure behind the projectile or vehicle is increased. This concept is the basis of gun technologies and is also seen in rocket technology as the ram accelerator [121–123]. A similar concept can be applied to laser propulsion. In airbreathing-laser propulsion, the lightcraft or its equivalent is launched in an open atmosphere. The laser-driven in-tube accelerator (LITA) [33,124] is a laser propulsion version of in-tube propulsion, with three categories, described in this section.

For gaseous LITA (G-LITA), the launch tube is prefilled with inert gas, e.g., argon or xenon, as the propellant. A repetitive laser pulse is sent to the launch tube either through its bottom or muzzle, then it is focused by a specially designed optic over the projectile and launch-tube wall combination. Figure 28 shows a design for rear incidence of the laser pulse.

Optical breakdown produces a laser-induced plasma that drives a laser-induced blast wave, a shock wave accompanied with a post-shock expanding flow. The pressure on the base of the centerbody is increased by shock wave reflection, thereby yielding a propulsive impulse. In this device, even the propellant gas is reusable. Experimental demonstration was done using a 25-mm-bore, 0.5-m- or 1.0-m-long LITA with a repetitively pulsed (RP) TEA CO_2 laser [125]. Argon, krypton, and xenon were used as the propellant gas. $C_m = 300$ N/MW was obtained using xenon.

Although G-LITA is an almost-reusable launch device, it has a drawback in its propulsion mechanism. With increasing projectile speed, the gas ahead of the projectile causes aerodynamic drag that limits thrust performance. To solve this problem, V-LITA [126] was

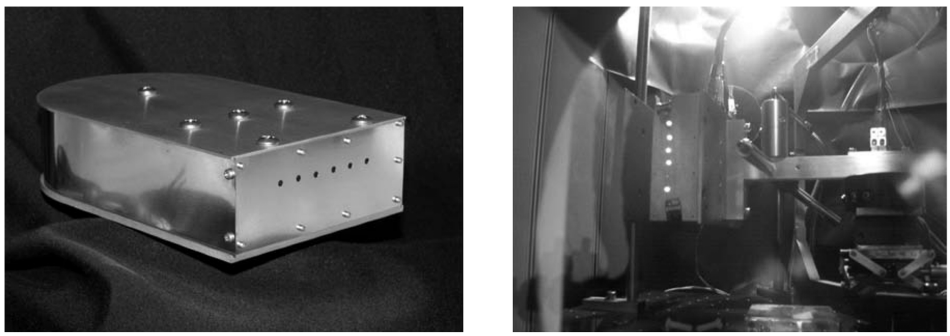

Fig. 25 The ms-LPT after assembly and during tests in vacuum. At right, the operating device is mounted on a torsion pendulum to measure thrust in vacuum (see [4]); used with permission of the American Institute of Physics, copyright 2007.

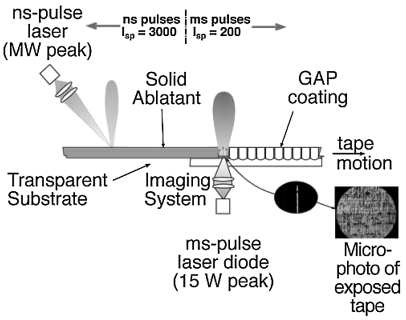

Fig. 27 Operating principles of the nanosecond and millisecond versions of the LPT.

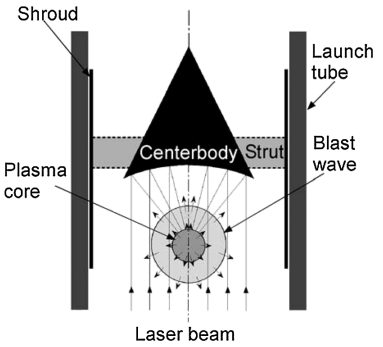

Fig. 28 G-LITA. An RP laser beam is sent to a primary mirror integrated with the vehicle forebody, then refocused to a spot just beneath the vehicle. The projectile is propelled up the guide tube by a sequence of laser-supported detonations.

developed, in which the launch tube is initially evacuated and a propulsive impulse is generated using laser ablation (Fig. 29).

The projectile has an onboard polyacetal (POM) ablator propellant. The nozzle-shaped lower part of the projectile acts as a parabolic mirror, focusing a laser beam sent from the bottom onto the bottom surface of the ablator rod, causing ablation and impulse generation. Vertical-launch demonstrations were conducted using a 25-mm-bore, 1-m-long acrylic launch tube [126]. TEA CO_2-laser pulses (10.6 μm wavelength) were applied to the target with energy up to 10 J/pulse at 50 Hz. Because of elimination of the aerodynamic drag, the momentum-coupling coefficient C_m was improved, reaching 1.5 kN/MW. However, the propulsion performance decreased with accumulating number of operations because of consumption of the ablator.

To further improve the V-LITA performance, a third type of LITA was developed at Nagoya University. This device also uses laser ablation, but the ablator is not onboard, it is on the launch-tube wall [wall-ablative LITA (WA-LITA)] (Fig. 30). The projectile and the launch tube have square cross sections. Opposing acrylic walls have guide grooves for the projectile, and the other pair of walls is made of POM. These walls are constrained in metal frames.

The upper part of the projectile has guide rails, and the lower part has a two-dimensional parabolic shape. A collimated laser beam sent through the launch-tube bottom is reflected onto the parabolas and is line-focused onto the ablator walls. This device has a geometrical advantage: the ablation plume from the wall is also reflected from the parabolas and directed back toward the launch-tube bottom.

The remarkable thing about WA-LITA is that both the energy source and the propellant can remain on the ground when this concept is scaled up.

In the device used for the demonstration [127], the launch tube had a 25×25 mm square inner cross section. The upper part of the launch tube was always connected to a 0.7 m^3 vacuum chamber that was evacuated below 20 Pa. POM [76] was the ablator. Two operation modes were examined. In closed-breech mode, the bottom of the launch tube was closed, and a C_m of 4 kN/MW was obtained with a 0.5-m-long launch tube. In open-breech mode, even the launch-tube bottom was connected to the same vacuum chamber through a separate duct. This simulates launch operation through an infinitely long launch tube. Since confinement of the ablation gas below the projectile was not obtained, C_m was much lower: 140 N/MW. Yet, the projectile was successfully lifted up with a constant C_m.

Related work was conducted in parallel. In the case of laser ablation on metal, impulse usually decreases with decreasing ambient-air pressure. This implies that ambient air acts as an additional propellant that is involved in the impulse generation through mechanical impedance matching. However, when POM is irradiated by a TEA CO_2-laser pulse, the impulse behaves in a complicated manner, as shown in Fig. 31 [76]. As in other materials, there exists an optimum fluence to maximize C_m.

Yet, the optimum fluence depends on the ambient pressure. At atmospheric pressure, C_m has a maximum with a fluence of 18 J/cm^2. However, at an ambient pressure of 10 kPa, C_m is decreased, becoming smaller than that with 8.5 J/cm^2. It is interesting that with 18 J/cm^2, C_m has a maximum at even lower pressure, lower than 0.1 Pa.

To understand the mechanisms of this unusual performance, impulse histories were measured using the velocity interferometer for any reflector (see Fig. 32) [128]. On one hand, in the atmospheric-pressure case, the impulse ceased to increase 1 μs after the laser-pulse initiation. As shown in Fig. 32c, the laser power at later times is absorbed by the laser-induced plasma, preventing pressure increase on the target surface. On the other hand, the impulse continued to increase almost twice as long as the former case when the ambient pressure was 0.01 Pa. In this case, no medium exists to absorb laser power.

Table 4 LPT ablatant performance survey [2,4][a]

Ablatant: absorber	C_m, N/MW	I_{sp}, s	η_{ab}, %	Φ, kJ/m^2	U_{opt}, kJ/g	U_{chem}, kJ/g	η_o	τ	F_{max}, μN
PVC:C	35	1530	26	58,400	1170	0	1.0	10 ms	——
GLYN:C	1280	116	73	1270	12.7	2.7	0.84	2 ms	118
GAP:dye	1050	218	112	7530	75	2.5	0.97	2 ms	168
GAP:C	3047	137	205	1270	12.7	2.5	0.84	2 ms	2800
Au	53	3660	96	640	33	0	1	5 ns	0.63

[a]η_o is the fraction of energy from optical (rather than chemical) sources, τ is pulse width, $\Phi = I\tau$ is the peak laser fluence on the target, F_{max} is maximum thrust obtained in the test series, and GLYN is polyglycidyl nitrate polymer.

Table 5 Liquid-fuel results

Pulse width τ, s	Wavelength, nm	Fluence, J · cm^{-2}	C_m, μN/W	I_{sp}, s	Splatter?
4.5 ns	1060	7400	73	682	Some
2 ms	916	160	470	201	No

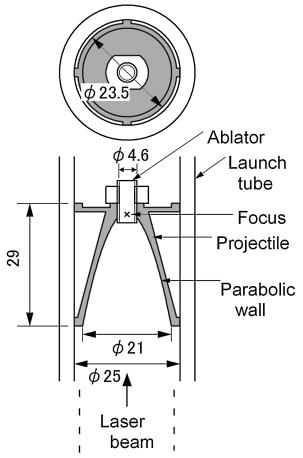

Fig. 29 LITA using an onboard ablator (V-LITA) (see [124] for related work).

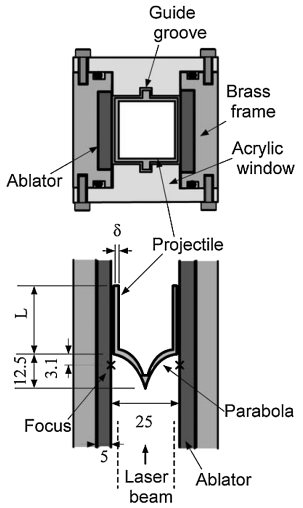

Fig. 30 LITA using an ablator on launch-tube walls, WA-LITA [127].

In Suzuki et al.'s [129] experiments (see Fig. 33), the impulse for the virgin target was much smaller than the value after several cleaning shots. With an accumulating number of laser pulses, a crater was formed on the target surface. If the depth-to-diameter aspect ratio was moderate, the crater acted as an aerodynamic nozzle, enhancing the impulse performance.

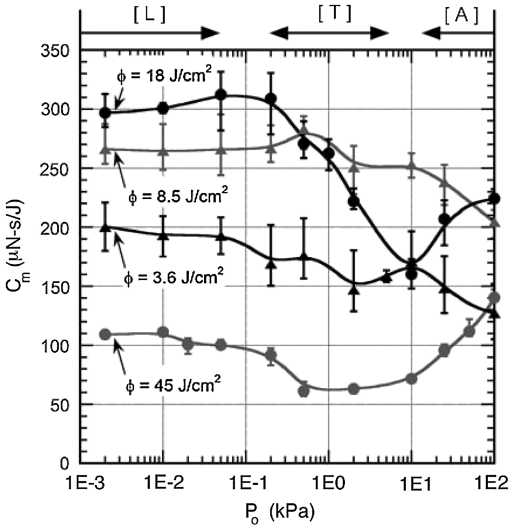

Fig. 31 C_m of POM vs pressure.

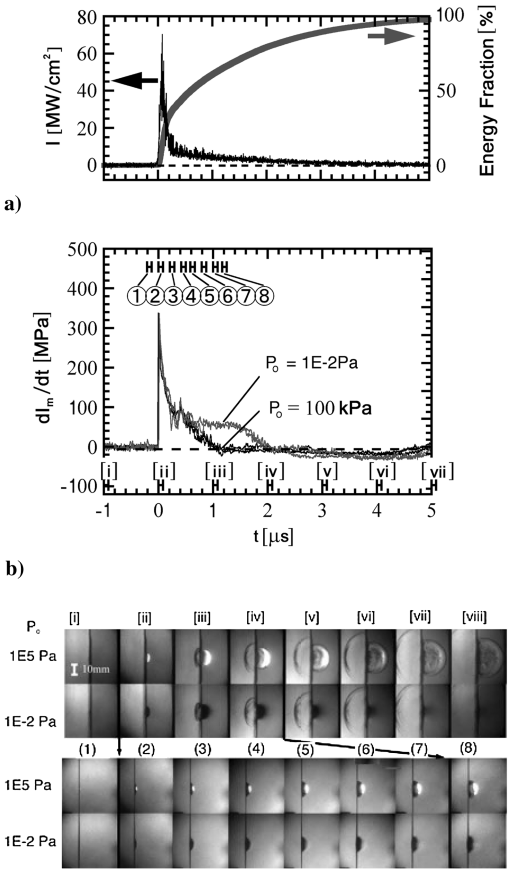

Fig. 32 Impulse generation processes on POM target with TEA CO_2 laser at 17:9 J/cm²: a) time variation of laser intensity and integrated energy fraction, b) time variation of overpressure that is measured with the target rear surface backed by the acrylic block, and c) framing schlieren images [128].

C. Hybrid Thruster Systems

1. Laser–Electric Hybrid Acceleration Systems

Schematics of laser–electric hybrid acceleration systems are given in Figs. 34a and 34b [130–134]. The basic idea of these systems is that the laser-ablation plasma induced by laser irradiation of a solid target is additionally accelerated by electrical means. Since any solid material can be used as the propellants in these cases, no tanks, valves, or piping systems are required for the propulsion system. Therefore, the system employing these techniques can be simple and compact. Because laser-ablation plasma can have a directed initial velocity of tens of kilometers/second, which will be further accelerated by electrical means, significant I_{sp} can be expected.

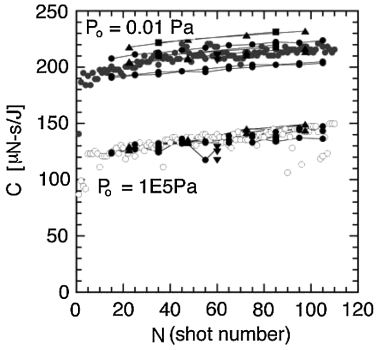

Fig. 33 Variations of C_m for different ambient pressure and number of laser pulses in a burst [129].

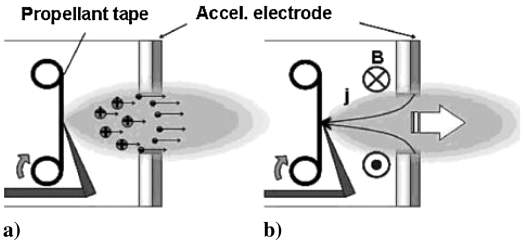

Fig. 34 Schematics of laser–electric hybrid acceleration systems: a) laser–electrostatic hybrid acceleration system and b) laser–electromagnetic hybrid acceleration system.

In the above hybrid cases, depending on different factors such as electrode configuration, plasma density, and electrical input power (voltage *x* current), acceleration mechanisms for the laser-ablation plasma can be classified into three types: 1) electrostatic acceleration, 2) electrothermal acceleration, and 3) electromagnetic acceleration, although type 2 usually occurs simultaneously with type 3. Especially for laser-ablation plasma, depending on laser conditions such as pulse energy, fluence, etc., plasma density and velocity distributions can be controlled over a wide range. Moreover, they can also be controlled through additional electric discharges.

By controlling a power source with optimized electrode configurations, each acceleration type can be accessed. Therefore, a propulsion system that is able to satisfy all the above acceleration regimes 1–3 can be achieved with one thruster configuration. This system enables a robust conversion between high-I_{sp} operation and high-thrust-density operation to match mission requirements. Laser–electrostatic hybrid and laser–electromagnetic hybrid accelerators are currently under investigation at Tokai University and are described in the following subsections.

a. Laser–Electrostatic Hybrid Acceleration. One of the laser–electric hybrid acceleration techniques employed in our studies is laser–electrostatic hybrid acceleration, in which laser-ablation plasma is further accelerated by an electrostatic field, shown in Fig. 34a. A focused laser pulse is irradiated onto a solid target or a propellant. Then laser-induced plasma or laser ablation is induced at an irradiated spot of the propellant surface. In laser ablation, first, electrons are accelerated from the surface, and then ions are accelerated through ambipolar diffusion and coulomb explosion. In the hybrid accelerator, such ions are further accelerated with an additional acceleration electrode. Because laser-induced plasma generated from the target surface having a directed initial velocity is further accelerated by an electrostatic field, fast ion emission and high specific impulses can be obtained [134].

b. Laser–Electromagnetic Hybrid Acceleration. Another concept being considered is laser–electromagnetic hybrid acceleration, a form of which is illustrated in Fig. 34b. After a laser beam induces plasma from a solid propellant between electrodes, an electric discharge is induced in this conductive region. As the current running between the electrodes is increased, the interaction between the current and self-induced magnetic field becomes significant, creating thrust. Authors have been developing both axial and rectangular electrode configurations [130–133].

Some examples of thrust performance of a rectangular laser–electromagnetic hybrid thruster with various propellants are shown in Fig. 35. Alumina showed the best performance, giving a maximum specific impulse of over 6000 s and thrust efficiency of over 20%, with relatively low energy input of less than 9 J.

c. Relativistic Laser-Driven Plasma-Acceleration System. The interaction of ultraintense laser pulses with solid targets leads to generation of fast particles, from x- and γ-ray photons to high-energy ions, electrons, and positrons [135–138]. In particular, an interest has developed in ion acceleration by compact high-intensity femtosecond lasers with potential applications for the initiation of nuclear reactions on a tabletop. Experiments now being carried out involve high-energy ions generated by the interaction of laser pulses with solid targets (Fig. 36). In this case, strong electrostatic fields can be generated through charge separation. The efficiency of the laser

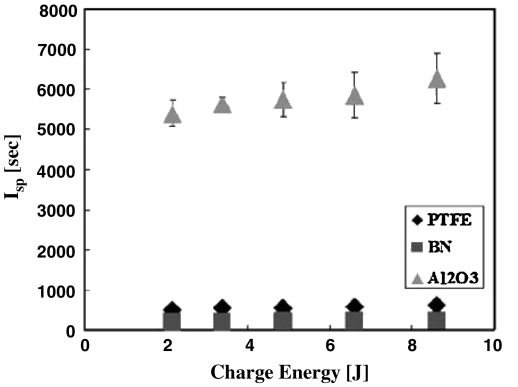

a) I_{sp} vs. charge energy

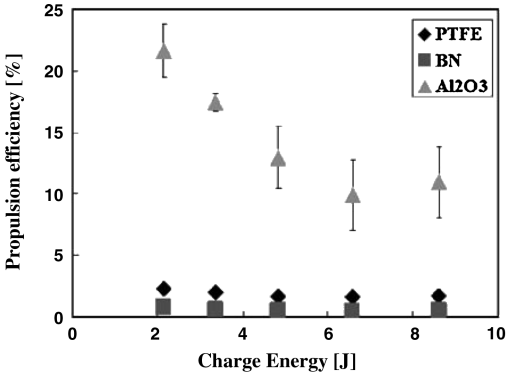

b) Propulsion efficiency vs. charge energy

Fig. 35 Typical results from rectangular laser–electromagnetic hybrid thruster for various propellants.

energy conversion into a high-energy electron component dominates these phenomena. Thermal expansion of the laser-driven plasma and ponderomotive electron expulsion constitute the most well-known examples of the electrostatic-field production.

Recent experimental and theoretical results of laser-driven plasma accelerators in various laboratories have shown that a maximum ion energy on the order of tens of mega electron volts can be generated. For a proton beam accelerated up to 58 MeV [137], its speed corresponds to $0.33c$, and $I_{sp} \sim 10$ Ms. Moreover, theoretical studies [138] predicted that a relativistic ion beam with velocity $0.87c$ and $I_{sp} = 55$ Ms is achievable with current laser facilities [139–142].

Although those accelerators were originally developed for use as igniters for inertial confinement fusion, we propose the use for space propulsion applications [139–142]. For propulsion applications based on the relativistic beams, extremely high I_{sp} can be expected through relativistic effects. Since no special nozzle or channel, but only a thin-film target, is needed for the collimated plasma beam

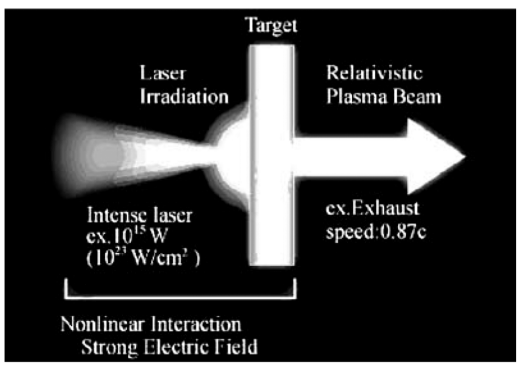

Fig. 36 Schematic illustration of relativistic laser–plasma acceleration.

formation, as shown in Fig. 36, the propulsion system employing this technique can be significantly simple and small.

d. Relativistic Very-High-Specific-Impulse Regime. Consider an element of exhaust plasma reaching a constant relativistic speed v_1 observed in the spacecraft frame I. Relations for the specific impulse $I_{\rm sp}^{(I)}$, momentum coupling efficiency $C_m^{(I)}$, and energy conversion efficiency $\eta_k^{(I)}$ of laser pulse energy to plasma kinetic energy observed in frame I are shown in Table 6. In the table, we use the Lorentz factor $\gamma_1 = 1/\sqrt{1 - v_1^2/c^2}$, also measured from the spacecraft frame [142]. These relations satisfy both nonrelativistic ($\gamma_1 = 1$) and relativistic ($\gamma_1 \gg 1$) conditions of exhaust velocities. Moreover, the nonrelativistic expressions are consistent with those obtained without the special theory of relativity.

Variations of thrust with input power for a constant energy-conversion efficiency of $\eta_k^{(I)} = 100\%$ are plotted in Fig. 37. In nonrelativistic conditions, it is shown that thrust with higher mass flow rate is larger for a given input power. Also, the thrust with even a small amount of mass flow of the propellant is much greater than that of the photon rocket. On the other hand, in relativistic conditions, it can be seen that the thrust approaches the value of the photon rocket for a constant input power, regardless of the mass flow rates. The relationship between the specific impulse and momentum-coupling coefficient is shown in Fig. 38. From the figure, it can be seen that in nonrelativistic conditions, C_m decreases as $1/I_{\rm sp}^{(I)}$. However, in relativistic conditions, the coupling coefficient approaches the value of $1/c$, which is identical to that for the photon rocket.

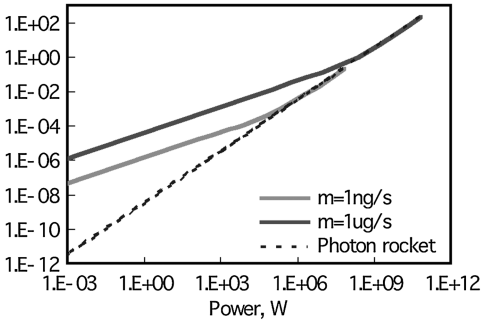

Fig. 37 Variation of thrust with input power for various propellant mass consumption rate under a constant energy-conversion efficiency of $\eta_k^{(I)} = 100\%$.

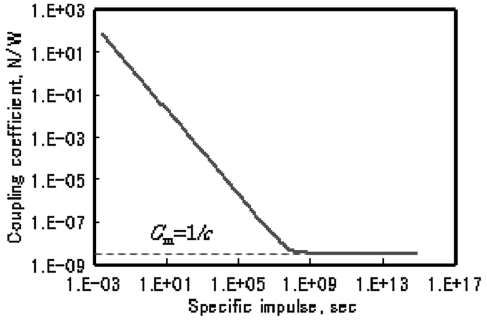

Fig. 38 Relation of specific impulse and momentum-coupling coefficient for a constant energy-conversion efficiency of $\eta_k^{(I)} = 100\%$.

2. Large-Scale Electromagnetic–Laser Hybrid Acceleration

There are several ways to lift a milliwatt-class-or-larger laser-driven thruster through the lower atmosphere to the ideal ~35 km starting altitude (Sec. VI.D). One of these is an electromagnetic launcher, or railgun. A system that combines a railgun and a laser-driven thruster is another type of hybrid thruster.

Hypervelocity launch was first demonstrated in the late 1970s [143]. The associated electrical energy cost is extremely low. For example, 1 kg launched to 8 km/s has a kinetic energy of 32 MJ. Assuming an electric system efficiency of 10%, the energy cost is only $7 from the typical electrical utility [144].

An electromagnetic launcher uses the Lorentz ($J \times B$) force and requires very large currents to be applied to parallel rails and, through sliding contacts, to a movable armature.

A Multidisciplinary University Research Initiative program was established in 2005 to study the scientific and technical issues involved in the launch to space of microsatellite payloads using an electromagnetic launcher. As part of this effort, the University of Texas (UT) built and tested a laboratory railgun, and Texas Tech University studied ways of reducing inductance and resistance by using a multistaged power-feed system (Fig. 39).

In addition, modeling of the thermochemical nonequilibrium flow of air over the hypersonic projectile with a coupled solution for the finite rate ablation and oxidation of the projectile nose-tip thermal protection system was undertaken at the Universities of Minnesota and New Orleans.

UT developed an approach to overcome the effects of plasma-induced vapor from low-cost epoxy-impregnated insulators that were used in earlier railguns [145]. They replaced the epoxy with high-purity alumina, which has a high vaporization temperature and good thermal conductivity. The main problem with ceramics of this type is their propensity to crack under tensile loading. Consequently,

Table 6 Comparison of relativistic and nonrelativistic expressions for relations of $\eta_k^{(I)}$, $I_{\rm sp}^{(I)}$, and $C_m^{(I)}$

	Expressions	Relativistic, $\gamma_1 \gg 1$	Nonrelativistic, $\gamma_1 = 1$
$\eta_k^{(I)}$	$[g_o/(\gamma_1+1)]C_m^{(I)}I_{\rm sp}^{(I)}$	$(g_o/\gamma_1)C_m^{(I)}I_{\rm sp}^{(I)}$	$(g_o/2)C_m^{(I)}I_{\rm sp}^{(I)}$
$C_m^{(I)}I_{\rm sp}^{(I)} \leq$	$(\gamma_1+1)/g_o$	γ_1/g_o	$2/g_o$
$C_m^{(I)} \leq$	$(\gamma_1+1)/\gamma_1 v_1$	$1/c$	$2/v_1$

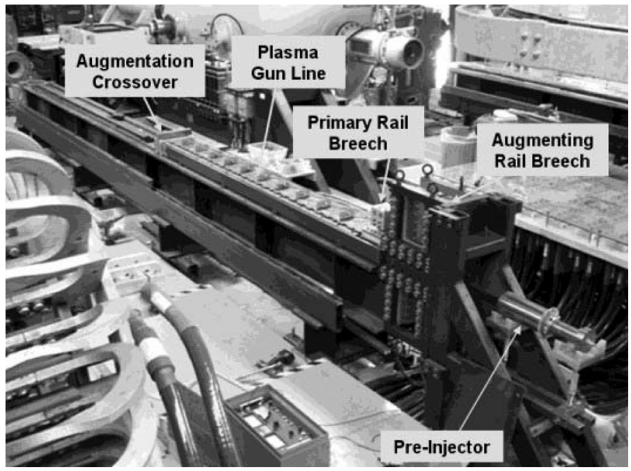

Fig. 39 University of Texas Institute for Advanced Technology railgun facility.

UT also redesigned the railgun structure to better withstand predicted forces and evacuated the railgun barrel to tens of torr to prevent aerodynamic drag on the projectile.

UT also replaced the traditional single-pair rail design with a double-pair design in which a considerably higher current (~800 kA) flows through an outer pair of rails than through the inner core rails (~160 kA). In this scheme, the propulsive force on the plasma is unchanged, but the radiated power from the plasma onto the inner bore insulators is reduced by a factor of approximately five.

Finally, UT mitigated startup damage caused by the plasma armature in the railgun breech by injecting the projectile with a modest initial velocity. To do this, they built a system that injected hot hydrogen from a controlled internal arc in a polyethylene capillary. Experiments demonstrated a preinjection velocity of ~1 km/s and

an ionization level high enough for safe triggering of the main accelerating discharge.

For their contribution, Texas Tech University developed a five-stage distributed power system using only plasmas to reach 11 km/s, with alumina and G-10 insulators.

D. Lightcraft

From the perspective of demonstrated beam-riding abilities, perhaps the most extensively explored laser propulsion concept to date is the lightcraft concept [3], in both its airbreathing and solid-ablation rocket modes (Figs. 40 and 41). A series of successful tests with lightcraft was demonstrated at the White Sands Missile Range in 1997 with the 10 kW pulsed CO_2 laser (Fig. 41). These experiments demonstrated the viability of this beam-riding pulse-jet vehicle concept. Key contributions to lightcraft research are 1) experimental and numerical investigations by Mead et al. [146], 2) theoretical studies on laser energy conversion by Larson et al. [147], and 3) laser propulsion launch trajectory simulations by Knecht et al. [148]. The goal of this work is to launch a laser propulsion vehicle into suborbital flight (e.g., vertical sounding-rocket trajectory). Static laboratory bench experiments were conducted with several lightcraft models. Companion studies of microthrusters for reaction control systems and orbit circularization are also underway. Laser propulsion engines have been bench-tested using both white and carbon-doped Delrin as the propellant. Larson et al. [147] examined the thermodynamics and efficiency of converting laser energy into propellant kinetic energy, in both solid-ablation rocket and airbreathing lightcraft engines under both equilibrium and frozen flow conditions. Trajectory simulations were performed by Knecht et al. [148] using the Optimal Trajectories by Implicit Simulation (OTIS) code; the studies assumed a vehicle propelled by a 1 MW ground-based laser at 10.6 μm, with a beam power capture ratio of 82%. Full-scale laser propulsion launches to low Earth orbit were simulated, with sequential airbreathing and rocket propulsion phases.

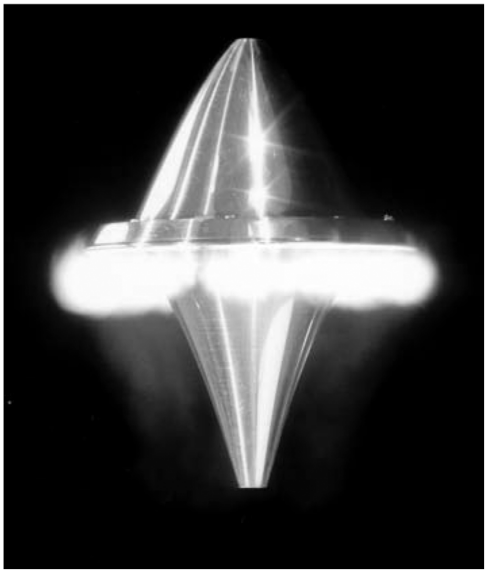

Fig. 40 Lightcraft vehicle at launch (see [29]).

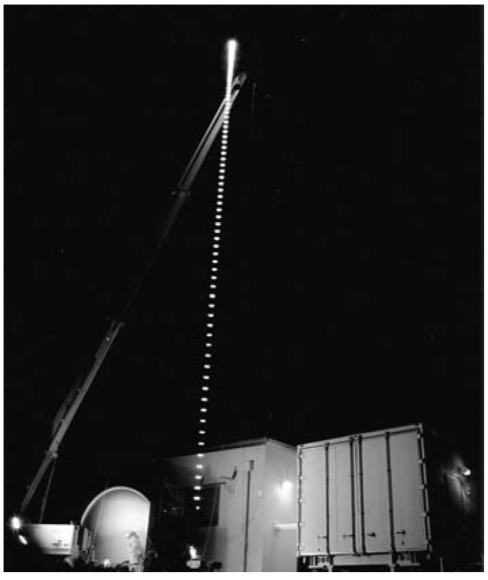

Fig. 41 Lightcraft vehicle in flight at White Sands (see [29]).

Wang et al. [149] applied an axisymmetric numerical model to study performance of a lightcraft engine. Wang et al.'s model included nonequilibrium thermodynamics, nonequilibrium air-plasma finite-rate kinetics, ray tracing, laser absorption and refraction by plasma, nonequilibrium plasma radiation, and plasma resonance. Their results were calibrated by experimental data [29] during laboratory and field tests of the airbreathing lightcraft engine. Wang et al.'s [149] model simulated only a stationary lightcraft engine with a closed air inlet, but could be extended to treat the vehicle flying at supersonic or hypersonic speeds, with an open ram air inlet.

Other scientists have been studying related concepts. Komurasaki et al. [150] studied both laser and microwave propulsion concepts in RP as well as CW modes. Their numerical studies investigated airbreathing, pulsed-laser-propulsion ramjet schemes [151] that closely resemble the lightcraft concept. These studies examined 1) alternative lightcraft forebody and shroud geometries at various Mach numbers, ambient pressures, and densities; 2) overall engine performance; and 3) the influence of laser focal ring location on the conversion efficiency of laser energy into thrust. One RP ramjet model simulated the time-dependent behavior of a single thrust pulse. Another model was built for CW laser rocket simulations to address wall heat losses, radiative losses, and laser-absorption efficiency. On the experimental front, Komurasaki et al. [150] linked a 10 J/pulse CO_2-laser system to a small-scale Mach 2 wind tunnel to investigate the laser–plasma expansion characteristics and blast-wave production efficiency of a focused beam in the freestream. A 2 kW-class CW model thruster was also built and tested to measure the efficiency of laser energy conversion into thrust.

Brazilian interest in laser propulsion began in the 1990s and was, until recently, focused largely on directed-energy air-spike (DEAS) research [152–155], which is relevant to hypersonic blunt forebodies. The concept uses laser energy to create a virtual spike that diverts hypersonic airflow away from a vehicle's flight path, reducing aerodynamic drag and heat transfer to the blunt forebody (Fig. 42).

Experimental results showed that hypersonic drag can be cut by as much as 40%. Investigations are underway to quantitatively assess DEAS disruptions of established flowfields and heat flux rates across blunt forebodies. Hypersonic shock tunnels at the Henry T. Nagamatsu Laboratory for Aerothermodynamics and Hypersonics (HTN-LAH) in Brazil are being linked to powerful CO_2 TEA lasers and have initiated ground-breaking laser propulsion experiments and related hypersonics research. HTN-LAH became one of the few research facilities in the world capable of simulating flow conditions

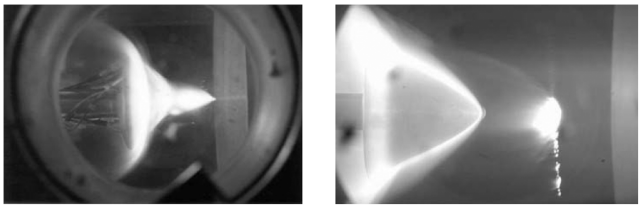

Fig. 42 Laser-induced DEAS hypersonic experiments in Brazil (see [155] for related work).

inside (and around) laser-driven ramjet and scramjet engines. The fabrication of several large-scale, two-dimensional laser propulsion engine segments are underway for such tests.

Recently, Australian researchers started research on laser propulsion, based on earlier tests of scramjet configurations similar to current U.S. lightcraft. These embodied a sawtooth-shaped leading edge to reduce heat transfer and increase the region in which stable inlet flow can be maintained. Moreover, tests of advanced scramjet engines up to Mach 10 have proven Buseman inlets that effectively channel airflow into combustors by streamline-following, inward-turning flowpaths that are relatively insensitive to flight conditions. Australian researchers will collaborate with the Brazilian scientists at HTN-LAH, where the Australian lightcraft designs will be tested.

E. High-Power Laser Propulsion Engines: The Aerospace Laser Propulsion Engine

Rezunkov et al. [156] demonstrated a novel 2-N-thrust laser-powered engine. The device employed laser propulsion with polymeric and polycrystalline propellants of CHO composition, i.e., laser-chemical propulsion, first identified as such by Liukonen [157]. It does not require optical windows.

As polymeric propellants, POM $[\text{-}CH_2O\text{-}]_n$, polyvinylchloride $[\text{-}CH_2CHCl\text{-}]_n$, polystyrene $[\text{-}C_8H_8\text{-}]_n$, and polycarbonate $[\text{-}C_{16}H_{14}O_3\text{-}]_n$ were tested. The first two of these are aliphatic hydrocarbons, for which thermal decomposition occurs at a moderate temperature (~200°C) [117]. The next two polymers include benzene rings, which redistribute absorbed laser radiation among their bonds, giving larger polymer decomposition temperature (~350°C).

CHO-chemistry crystal materials were also investigated: metaldehyde C_2H_4O, carbamoyl hydrazine CH_5N_3O, oxybenzoic acid $C_7H_6O_3$, and dihydroxy-benzene $C_6H_6O_2$. All of these agents are colorless materials with a moderate melting temperature and are used in the pharmaceutical and food industries [158].

The experiments showed that a momentum-coupling coefficient C_m associated with laser-chemical propulsion differs from that for conventional laser propulsion by a factor [159]

$$K = 1 + (BQ/A)(I\lambda\sqrt{\tau})^{-1/4} \tag{43}$$

In Eq. (43), $Q = Q_{\text{det}} + Q_{db}$. For the polymeric propellants, the factor varies within the interval $1.75 \le K \le 3.12$ (see curve 1 in Fig. 43) and varies within $3.1 \le K \le 6.5$ for polycrystalline propellants (curve 2). Dihydroxy-benzene and carbolic acid do not follow the character of these experimental data.

The experiments also showed that the linear polymer POM demonstrates a high coupling coefficient of $C_m = 270$ N/MW, with detonation being the dominant part of mechanical impulse imparted to the target. The propellant absorption spectrum well matches the CO_2-laser radiation spectrum via C-O-C valence vibrations. Polycarbonate, an oxygen-containing polymer with a linear aromatic structure, has low absorption of CO_2-laser radiation via deformation vibration of C-H links and, consequently, has a small detonation component of mechanical impulse ($C_m = 125$ N/MW). Such linear polymers as polystyrene and polyvinylchloride also did not demonstrate high efficiency of the laser propulsion production ($C_m = 130$ and 180 N/MW, respectively), because the detonation component is absent completely at laser ablation of these polymers.

For flight experiments, Delrin was the more effective propellant. The aerospace laser propulsion engine (ASLPE) (Fig. 44) was used in demonstration flight experiments using both RP and CW CO_2 lasers [159,160]. The engine was designed to separate the functions of beam concentrator and engine nozzle. The ASLPE consists of an optical system to collect laser power and match the laser beam and beam concentrator apertures, a beam concentrator unit, and a coaxial nozzle (Fig. 45) [156]. The beam concentrator consists of two mirrors: Mirror R_1 is a reflecting cone of rotation, the generatrix of which is a short-focus parabola. Mirror R_2, the axis of symmetry of which coincides with that of R_1, is a figure of rotation and is arranged so that its focal region F coincides with that of the first mirror, and its image is located in a region of laser breakdown of a propellant LB. The nozzle is made of two units: a mechanical impulse receiver behind the first mirror and a jet nozzle N, arranged at a small distance from the impulse receiver so that there is a slit S between the receiver and the nozzle, which is used as the laser radiation input.

The ASLPE model was first tested with an RP CO_2-laser beam, but the model can be easily transformed for CW laser operation. The RP CO_2 laser [161] was operated at 50 Hz pulse repetition rate, 120 J pulse energy, and 6 kW average laser power. The model was arranged on a frame that moved on two parallel wires stretched along the range, using two pairs of wheels. Total mass of the model and frame was 150 g. The model moved toward the laser beam while increasing its altitude above a floor at a 12 deg incline angle. Flight time was 3 s.

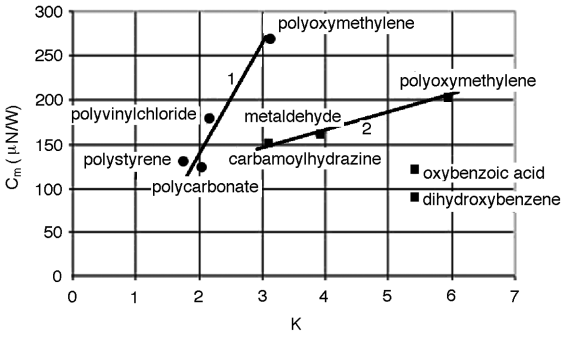

Fig. 43 Momentum-coupling coefficient C_m as a function of the coefficient K for the a) polymeric and b) polycrystalline CHO propellants.

Fig. 44 Photograph of ASLPE tested in the experiments.

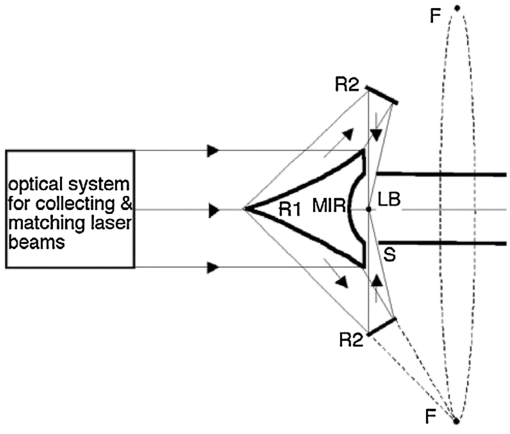

Fig. 45 ASLPE optics design (see [156]); used with permission of the American Institute of Physics, copyright 2007.

A 20 mm pill of POM propellant was placed in the focal region of the beam concentrator.

The ASLPE achieved 3–4 m/s maximum velocity in RP laser free-flight tests, maximum acceleration of 0.4–0.5 g, maximum momentum-coupling coefficient of 250 N/MW, and 1.3–1.5 N maximum thrust.

For lockdown thrust tests with a CW CO_2 laser, the ASLPE model was modified [6] by placing a 4-mm-diam Delrin rod on axis inside the model. To stabilize the continuous optical discharge (COD) [162] ignited close to the Delrin surface, airflow out of the beam concentrator top was supplied to the nozzle. The flow velocity was 20 m/s in the COD ignition area, which corresponded to a stable discharge regime at 10 kW laser power. The test duration was 1.2 s, determined by consumption of the Delrin rod. Figure 46 shows video frames from the test. Analysis of the video shows the exhaust jet has a pulsating character. That was confirmed by measurements of thrust dynamics using a strain sensor. Maximum thrust of 2 N was achieved in these experiments.

The flight experiments demonstrated reliability of the aerospace laser propulsion engine, which can be used in practical applications based on CO_2-laser/chemical propulsion.

VI. Advanced Concepts

A. Kilowatt-Level Liquid-Fueled Laser–Plasma Engine

A kilowatt-level laser–plasma engine has been proposed [47]. This would use the liquid-fuel delivery system illustrated in Fig. 47 and low-mass, 100 W, diode-pumped fiber lasers [163] to illuminate the fuel.

The design uses the same principles employed in laser welding and cutting to avoid target blowback to the illumination optics. Gas flow through an illumination head in which the mean free path for a backscattered particle is less then the distance to the optics solves the problem. In space, the flow required to provide the required 1.0 Pa pressure through the 600 μm orifice of the delivery channel is only 30 g per year of operation.

This engine assumes achievement of 3660 s I_{sp} on liquids, via the viscous-fluids approach. Stable viscosity can be achieved by dissolving polymerized GAP in ionic liquids, which have vanishing vapor pressure and are already used in electric propulsion engines for spacecraft. Performance of the proposed engine is shown in Table 7.

B. Extremely High C_m

Momentum-coupling coefficients approaching 10 kN/MW have been obtained using specially designed targets. Yabe et al. [45,49] used variations of a confined liquid target overlying an absorbing substrate to generate very large C_m by deliberately inducing splashing (Fig. 48). For this device ejecta velocity is low, but the momentum per laser joule is very high. In the equation shown in the figure, t is the repetition interval, σ is the surface tension, ρ is the density of water, and R is the radius of the capsule. Phipps et al. [44] got similar results with a layered target (Fig. 49) comprising glass overlying the absorbing substrate. Of course, these results featured I_{sp} from 1 to 10 s, meaning ejecta velocities of a few meters/second. By Eq. (11), a very high penalty is paid in fuel lifetime (which is proportional to I_{sp}^2) for using such low values. Applications of the Yabe et al. [49] target are to situations in which water can be continuously scavenged from the environment.

Data points for these tests, which achieved C_m values of 5–15 kN/MW, are shown on the extreme-left-hand side of Fig. 6. It should also be recalled at this point that Sasoh [33] obtained $C_m =$ 4 kN/MW in the LITA device (Sec. V.B), and that the LPT routinely achieves 3 kN/MW (Sec. V.A) with much higher I_{sp}, which is necessary for applications in which fuel must be carried onboard.

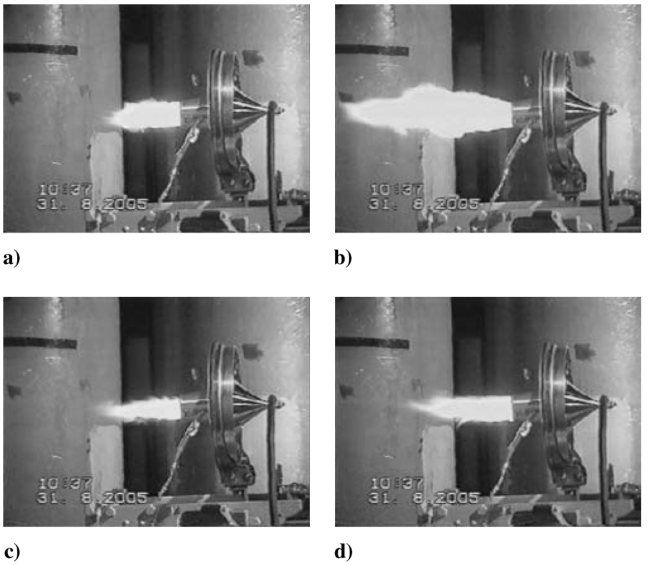

Fig. 46 Photographs of the CW ASLPE in operation at a) $t = 0.01$ s, b) 0.08 s, c) 0.40 s, and d) 1.1 s (see [156] for related work); used with permission of the American Institute of Physics, copyright 2007.

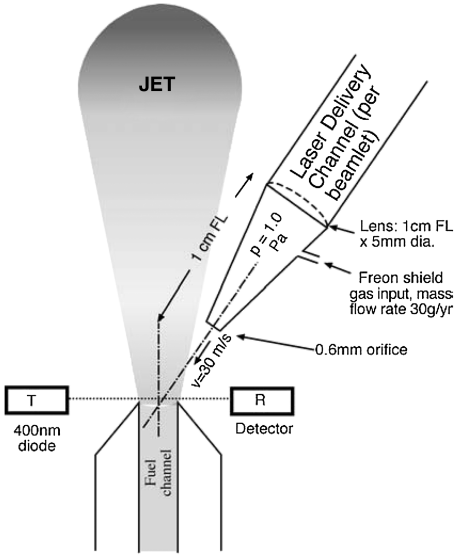

Fig. 47 Beam delivery system. High-intensity-laser energy with millisecond or nanosecond pulse durations makes a variable-I_{sp} jet on a liquid target. A diode transmit/receive (T–R) pair provides a control signal for the fuel pump (see [47]); used with permission of the American Institute of Physics, copyright 2009.

C. Orion

One result of 35 years of space activity is that there are now several-hundred-thousand pieces of space debris larger than 1 cm in near-Earth orbit. Debris in the 1–10-cm-size range are especially hazardous to near-Earth spacecraft such as the International Space Station (ISS), because they are not tracked. If all space launches in history had occurred easterly at the equator with zero eccentricity, space debris would not be a problem. As it is, a typical LEO object sees an impact velocity spectrum that peaks at 12.5 km/s, a velocity at which a penny has the same kinetic energy as a Volkswagen Beetle at 50 mph. Very small debris can make a hole in the ISS large enough that it cannot be patched before air pressurization is lost. Such an event has a 2–10% chance of occurrence over 10 years [37]. Ram pressure causes low-altitude debris ($h_E < 300$ km) to reenter in a matter of months or days. Higher-altitude debris ($h_E > 1000$ km) remains in orbit for 10,000 years.

Laser space-debris removal uses a high-intensity pulsed laser beam to ablate (not pulverize) a fraction of the debris itself in an orientation such that the debris is slowed sufficiently to reenter the atmosphere and burn up. Schall's [165] approach used an orbiting laser station. This approach has the advantage that the laser range can be small (tens of kilometers) because of the large area per unit time being swept out at orbital velocity. Smaller range also means the

Table 7 Anticipated liquid-fueled engine performance

	High I_{sp} mode	Low I_{sp} mode
	Engine parameters	
Motor mass	10.5 kg	10.5 kg
Fuel mass	69.5 kg	69.5 kg
Fuel type	Energetic liquid polymer	Energetic liquid polymer
No. of fiber lasers	18 (100 W max optical each)	18 (100 W max optical each)
I_{sp}	3660	116
Thrust at 3 kWe input	57 mN	6.48 N
RMS thrust noise	1%	1%
Electrical/optical efficiency	40%	60%
Mass usage rate	1.6 mg/s	5.7 g/s
Lifetime impulse	2.5 MN · s	79 kN · s
System C_m	19 μN/W	2.2 mN/W
Thrust efficiency	34%	123%
P_{in} (electrical)	3 kW	3 kW
Δv for 180 kg spacecraft	17.5 km/s	555 m/s
	Fiber laser amplifiers	
Time-averaged optical power	1800 W	1200 W
P_{peak} (optical), each	1 MW	670 W
Pulse duration	10 ns	1 ms
Pulse energy, EA laser	1 mJ	670 mJ
Pulse repetition rate	10 kHz	100 Hz

diffraction-limited spot diameter of the laser can more nearly match the size of the debris. Both effects lead to modest laser-pulse energy.

Phipps et al. [37,164] considered a ground-based laser system that, together with a several-meter-diameter beam director, would accomplish the same purpose (Fig. 50). Laser range (1500 km) is much larger than in the Schall [35] concept, leading to a laser spot size that is generally larger than the target. This, in turn, requires a larger pulse energy (1 to 10 kJ), but because mass still costs \$20,000/kg to put in orbit (Sec. VI.D), such a large system can be built on the ground at an overall competitive cost. A NASA validation study of this Orion concept [166] concludes,

> The capability to remove essentially all dangerous orbital debris in the targeted size range is not only feasible in the near term, but its costs are modest relative to the likely costs to shield, repair, or replace high-value spacecraft that could otherwise be lost to debris impacts for debris particles greater than 1 cm in size.

The original concept used a 1.06 μm, 15 kJ, 10 ns laser with 30 kW average power. The existing cloud of 1–10 cm debris could be reduced by 80% in two years using the system, which would cost on the order of \$100 million to build [167]. Later versions of the idea that used 1 ps pulses required much less pulse energy (150 J) and average power (10 kW), resulting in a factor-of-7 predicted cost savings [168] for the laser alone.

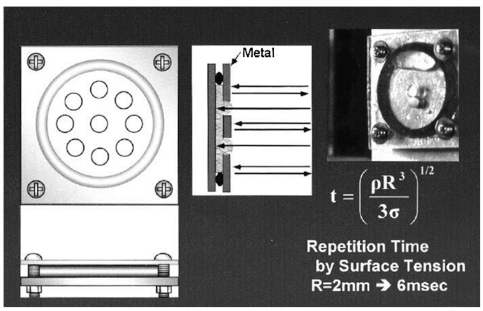

Fig. 48 Yabe et al. [49] water cannon achieved 10 kN/MW in air. This is a capsule filled with water, backed by an absorbing plate. Laser light enters through the small hole in the capsule window (upper right) and creates a plasma on the backplate that drives out a drop of water. This figure was provided by T. Yabe and is used with his written permission.

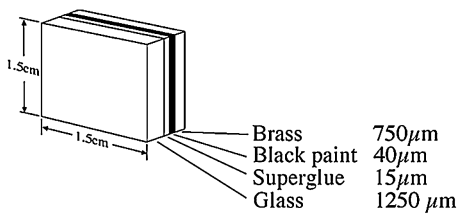

Fig. 49 Layered target for [42] tests achieved $C_m = 5$ kN/MW in vacuum. In this case, it is the glass plate, rather than water, which is launched at low velocity when intense laser light creates a plasma on the absorbing backplate.

D. Laser Launch into LEO

The way we send things to space from Earth is expensive, energy-inefficient, and polluting. Present-day costs of raising mass from the Earth's surface into LEO with chemical rockets is about \$20,000/kg (Table 8). This cost, equivalent to the cost of gold, dominates all other considerations relating to spaceflight, limiting what we consider to be possible. Part of the reason is the low I_{sp} available with chemistry. The space shuttle's main engine can produce only 465 s (v_E = 4.56 km/s) [169]. This limit is fundamental and will not change with improvements in engine materials. Larger I_{sp} values (exit velocity $v_E \gg 5$ km/s) at high thrust are accessible only by laser ablation, for which target temperatures can be more than 1E6 K for nanosecond-duration pulses.

Phipps and Michaelis [9], using an innovative design for a high-power laser system appropriate for launching large payloads [170], showed that there is an optimum set of parameters for laser space propulsion that can reduce the cost of lifting mass to LEO nearly a hundredfold from the Table 8 level.

Figure 51 emphasizes that rapid launch is the key reason for the reduced cost. When a curve for a launch frequency typical of the shuttle is included, it is shown that cost becomes greater than current costs (\$50,000/kg for 0.01/day vs \$400/kg for 5/day). Laser launching is *uniquely* adaptable to high launch frequency, whereas chemical rocket launches, even given extensive development, have never shown that capability because of the low mobility of the associated mechanical infrastructure. Cost is based on Eq. (44), derived for flight in vacuum [60]:

$$C = \frac{W}{m} = \left[\frac{(1 - m/M)}{(m/M)}\right] Q^* = \frac{v_E}{C_m}\left[\exp\left(\frac{v_{\mathrm{LEO}} + g_o t_{\mathrm{LEO}}}{v_E}\right) - 1\right] \tag{44}$$

which is a simplification that gives results that differ little from those of detailed simulations beginning from launch at $h_E = 35$ km

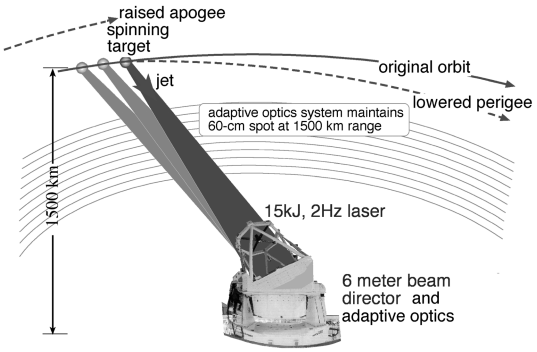

Fig. 50 Operating principle of the Orion laser space-debris mitigation concept, historically, the second of three to be so-named. Debris must be shot while rising at low azimuth. Many shots are required, in general. Spinning debris averages the thrust vector to that illustrated. Pushing up on the target and retarding the target both have the effect of lowering perigee.

Table 8 Present-day launch costs to LEO [39]

Launch system	Minimum cost, $/kg
Rockot	10,000
Shuttle	12,000
Taurus	20,000
ISS, commercial	22,000
Pegasus XL	24,000
Long March CZ-2C	30,000
Athena	41,000

(Fig. 52). In Eq. (44), t_{LEO} is the time required to reach LEO. Simulated flights shown in the figure featured 1 MW laser power, initial mass $2.5 < M < 51$ kg, polymeric ablators, and flight times of 200 s (round spots) and 400 s (square spots). The 35 km launch altitude can be achieved with high-performance aircraft, balloons, or an electromagnetic first stage (Sec. V.C.2). Ablation efficiency $\eta_{\mathrm{ab}} = 1$ is assumed here, a value justified for GAP (Sec. V.A). Delivered mass ratio m/M for the optimum C_m was 11%, nearly three times what the NASA shuttle achieves. For putting mass into LEO, this cost minimizes at about 100 MJ/kg. The energy cost can, in turn, be related to dollar cost (Fig. 51) using the economic analysis in [9].

The parametric behavior shown in Fig. 51 occurs because the costs of personnel and facility amortization, which depend linearly on time, easily outweigh the cost of consumables and energy on the ground when launches are infrequent. The left side of the curves is dominated by high laser cost and the right side is dominated by high optical system cost.

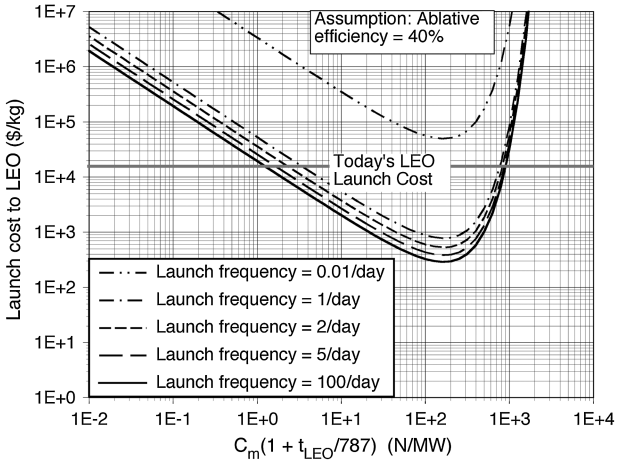

Fig. 51 Unit cost of laser launching a large payload to LEO using a repetitively pulsed laser. Costs are based on Eq. (44) with $\eta_{\mathrm{ab}} = 40\%$. The 0.01/day launch-frequency plot emphasizes the importance of launch frequency when determining cost (see [9] for related work).

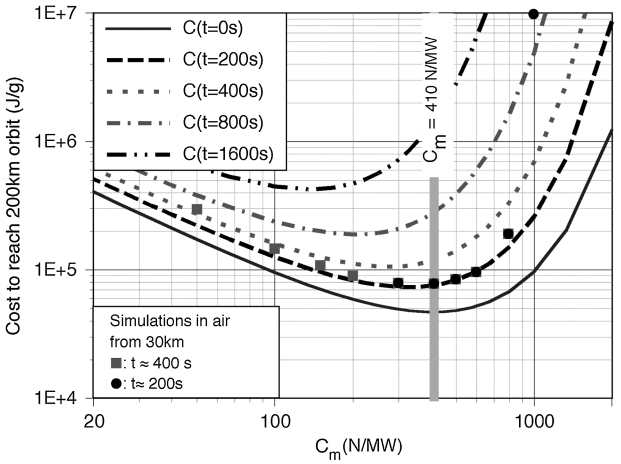

Fig. 52 Results of a series of detailed flight simulations [60] through a real atmosphere [166]. Energy costs predicted by Eq. (44) (solid and dashed curves) show good agreement with the simulation results.

Several kilograms can be delivered to LEO using ablative propulsion with a 1 MW laser. Present energy costs are about 3¢;/MJ at retail on the ground. Accordingly, at 100 MJ/kg, it ought not to cost a great deal more than $\$3/\eta$/kg to reach LEO, where η is the product of all efficiencies intervening between the wall plug and the kinetic energy of the laser-ablation rocket exhaust. That this cost can be as little as $300/kg makes sense even if η is as small as 1%, which is a very pessimistic assumption.

VII. Promise for the Future

A. One to Two Years

The first practical space application of LAP is already built, tested, and awaiting a flight: the laser–plasma thruster (Sec. V.A). This could occur within one–two years.

The first application to have a large effect on the Earth's space environment will be the Orion system for clearing near-Earth space debris. This application is important because debris is still being added to the near-Earth environment, and we can approach an instability in which long-term access to space is denied and present assets are threatened by fratricidal collisions among the debris. Several agencies are considering funding an Orion demonstration in the near future, but full implementation will take at least five years because of the infrastructure that must be built.

It is hoped that offensive military applications in space will be minimal. A peaceful application of the Orion technology is the option called *deflect to protect*, in which a smaller laser mounted on an asset such as the ISS protects itself by deflecting a debris object on detection.

B. Two to Ten Years

The lightcraft (Sec. V.D) is the first laser-powered device to fly in the atmosphere and, with certain material modifications, could possibly endure a flight through the atmosphere and into LEO. Depending on funding, practical realization of the lightcraft could take 2–10 years, because it is still orders of magnitude away from the required operating range, and performance over that range remains to be proven. Alternatively, an airbreathing lightcraft could act as the first stage of a laser-propelled flyer with a second stage optimized for spaceflight. A railgun (Sec. V.C.2) could also function as this first stage. Studies of performance in this second stage of flight above 30 km altitude [60] have shown delivered mass ratios $m/M = 0.32$, which is far higher than those in present practice.

C. Five to Ten Years

Within five years, it is easily possible to build megawatt-class repetitively pulsed lasers and launch vehicles that can take ~5 kg payloads to LEO, for assembly of larger objects there.

Also within a five-year time frame are laser orbital transfer vehicles (LEO to geosynchronous Earth orbit) and efficient vehicles powered by an orbiting mothership for a Mars sample return.

In the 5–10-year time frame, laser–electromagnetic hybrid devices (Sec. V.C.1.a) may take over interplanetary missions, because I_{sp} greater than 6000 s has already been demonstrated (Fig. 35). Kilowatt-level newton-thrust liquid-fueled engines can revitalize satellite propulsion, with instantaneously variable I_{sp} and can complement Hall thrusters because of their ability to generate large C_m at low I_{sp}, precisely matching a Hall-thruster deficit. They can also compete with ion thrusters for outer-planet research and beyond (Sec. VI.A). Engine design concepts such as the ASLPE (Sec. V.E) may well play a role.

D. Fifteen to Twenty Years

In the 15–20-year time frame, direct launch into LEO with large payloads (1 t) will be possible if the investment is put in place now.

The initial investment will be equivalent to that of the ISS, but the payoff might be greater.

VIII. Conclusions

The way we send things to space now is very expensive. Present-day costs of raising mass from the Earth's surface into low Earth orbit (LEO) with chemical rockets is about $20,000/kg. This cost, equivalent to the cost of gold, dominates all other considerations relating to spaceflight, limiting what we consider to be possible. But it need not be so. As Eugen Sänger said in concluding his *Aero Digest* paper [171] more than 50 years ago,

> No, we do not have to resign and humbly fold our hands in our laps. The infinite universe is small enough to be open to the initiative of every one of us, open to its ultimate boundaries, everything accessible to human beings.

We believe it is possible to reduce the cost of lifting mass to LEO nearly a hundredfold (Fig. 51) using laser-ablation propulsion. By doing so, we will correspondingly reduce the costs of launching payloads to the solar planets and beyond. At $300/kg, a spin around the Earth comes within a factor of 3 of the cost of a flight on the Concorde when it was still flying, adjusted for inflation. And, of course, 10 spins are as inexpensive as one.

Advantages of laser launch to LEO are many, and this application is believed to offer a quantum shift in access to space. It has already been demonstrated in flights and has significant research on real hardware. These advantages include the following:

1) Drastically reduce the cost of unmanned exploration of the solar system by permitting assembly of larger space vehicles on orbit from many small ground-based launches. This approach is necessary because lasers we can build today with $\sim$1 MW average power can propel only small payloads on the order of 6 kg into LEO at one time [60].

2) In ambient atmosphere, offer the possibility of optimally efficient propulsion by adjusting C_m and I_{sp} on the fly to match gravity and atmospheric density. The importance of this flexibility (so-called constant-momentum propulsion [7]) cannot be over-emphasized.

3) In vacuum, offer the possibility of I_{sp} values well beyond those available from chemical propulsion for larger delivered mass ratio over interplanetary and interstellar distances, possibly competing in the future with ion thrusters and other high-I_{sp} electric propulsion systems.

4) The cost of energy and of energy converters on the ground is extremely small. In space, a component such as a valve or a turbine costs as much as the same mass of gold, just by being in space, without even considering the usual highly inflated development and space qualification costs.

5) Ultrashort pulses can offer advantages by reducing the size of transmitting apertures required to achieve plasma formation on laser-ablation targets at large range in space, because of the lower fluence threshold for short pulses.

With these payoffs in view, it is worthwhile to provide a time frame in which we expect to see practical applications of LAP, moving from the immediate future to the far future. These predictions are the best guesses of the lead author and represent what could be accomplished, in his view, with a significant, dedicated, well-funded LAP technology development effort, timed from the start of such funding.

Acknowledgment

This paper is dedicated to the memory of Arthur Kantrowitz (1913–2008). The authors sincerely thank Gregory Spanjers for his interest in this topic and for his encouragement during the writing of this review.

References

[1] Pakhomov, A., Thompson, M., Swift, W., Jr., and Gregory, D., "Ablative Laser Propulsion: Specific Impulse and Thrust Derived from Force Measurements," *AIAA Journal*, Vol. 40, No. 11, 2002, pp. 2305–2311.
doi:10.2514/2.1567

[2] Phipps, C. R., Luke, J. R., and Helgeson, W. D., "3 ks Specific Impulse with a ns-Pulse Laser Microthruster," 29th International Electric Propulsion Conference, Paper 319, Princeton, NJ, 2005.

[3] Mead, F. B., Jr., Myrabo, L., and Messitt, D., "Flight Experiments and Evolutionary Development of a Laser Propelled, Trans-Atmospheric Vehicle," *High-Power Laser Ablation I*, Proceedings of SPIE: The International Society for Optical Engineering, Vol. 3343, SPIE, Bellingham, WA, 1998, pp. 560–563.

[4] Phipps, C. R., Luke, J. R., Helgeson, W., and Johnson, R., "Performance Test Results for the Laser-Powered Microthruster," *Beamed Energy Propulsion*, AIP Conference Proceedings, Vol. 830, American Inst. of Physics, Melville, NY, 2006, pp. 224–234.

[5] Phipps, C., Luke, J., and Helgeson, W., "Laser-Powered, Multi-Newton Thrust Space Engine with Variable Specific Impulse," *High-Power Laser Ablation VII*, Proceedings of SPIE: The International Society for Optical Engineering, Vol. 7005, SPIE, Bellingham, WA, 2008, pp. 1X1–1X-8.

[6] Moses, E., "Multi-Megajoule NIF: Ushering in a New Era in High Energy Density Science," *High-Power Laser Ablation VII*, Proceedings of SPIE: The International Society for Optical Engineering, Vol. 7005, SPIE, Bellingham, WA, 2008, pp. 0F1–0F11.

[7] Larson, C. W., Mead, F. B., Jr., and Knecht, S. D., "Benefit of Constant Momentum Propulsion for Large Δv Missions—Applications in Laser Propulsion," 42nd Aerospace Sciences Meeting, AIAA Paper 2004-0649, Reno, NV, 5–8 Jan. 2004.

[8] Rezunkov, Y., Safronov, A., Ageichik, A., Egorov, M., Stepanov, V., Rachuk, V., Guterman, V., Ivanov, A., Rebrov, S., and Golikov, A., "Performance Characteristics of Laser Propulsion Engine Operating Both in CW and Repetitively Pulsed Modes," *Proceedings of the Fourth International Symposium on Beamed Energy Propulsion*, AIP Conference Proceedings, Vol. 830, American Inst. of Physics, Melville, NY, 2006, pp. 3–13.

[9] Phipps, C., and Michaelis, M., "LISP: Laser Impulse Space Propulsion," *Laser and Particle Beams*, Vol. 12, No. 1, 1994, pp. 23–54.
doi:10.1017/S0263034600007217

[10] Bae, Y., "First Demonstration of Photonic Laser Thruster (PLT)," *High-Power Laser Ablation VII*, Proceedings of SPIE: The International Society for Optical Engineering, Vol. 7005, SPIE, Bellingham, WA, 2008, pp. 10-1–10-14.

[11] Tsander, F., "Flight to Other Planets," *Development of Russian Rocket Technology*, edited by Y. Moshkin, Mashinostroyeniye Press, Moscow, 1973 (in Russian).

[12] Tsiolkovsky, K., "Plan of Space Exploration," *Exploration of the Universe with Reaction Machines: Exploring the Unknown*, NASA History Series. NASA SP 4407, Washington, D.C., 1995 (English translation).

[13] Oberth, H., "Die Rakete zu den Planetenräumen," Oldenbourg Verlag, Munich, 1923.

[14] Goddard, R., "A Method of Reaching Extreme Altitudes," *Smithsonian Miscellaneous Collections*, Vol. 71, No. 2, 1919

[15] Sänger, E., "Zur Theorie der Photonenraketen," *Probleme der Weltraumforschung*, International Astronautical Federation, Zürich, 1954.

[16] Sänger, E., "Strahlungsquellen für Photonenstrahlantriebe," *Astronautica Acta*, Vol. 5, 1959, pp. 15–25

[17] Rubbia, C., "A Nuclear Propulsion Concept," 6th International Symposium on Propulsion for Space Transportation of the 21st Century, Association Aéronautique et Astronautique de France, Paper S24.0, Versailles, France, 14–17 May 2002.

[18] Myrabo, L., Knowles, T., Bagford, J., Seibert, D., and Harris, H., "Laser-Boosted Light Sail Experiments with the 150 kW LHMELII CO_2 Laser," *High-Power Laser Ablation IV*,Proceedings of SPIE: The International Society for Optical Engineering, Vol. 4760, SPIE, Bellingham, WA, 2002, pp. 774–798.

[19] Herbeck, L., Eiden, M., Leipold, M., Sickinger, C., and Unckenbold, W., "Development and Test of Deployable Ultralightweight CFRP-Booms for a Solar Sail," *Proceedings of the European Conference on Spacecraft Structures, Materials and Mechanical Testing*, European Space Research and Technology Centre, Noordwijk, The Netherlands, 2001, pp. 107–112.

[20] Marx, G., "Interstellar Vehicle Propelled by Terrestrial Laser Beam," *Nature*, Vol. 211, No. 5044, 1966, pp. 22–23.
doi:10.1038/211022a0

[21] Redding, J. L., "Interstellar Vehicle Propelled by Terrestrial Laser Beam," *Nature*, Vol. 213, No. 5076, 1967, pp. 588–589.

doi:10.1038/213588a0
[22] Simmons, J., and McInnes, C., "Was Marx Right? Or How Efficient are Laser Driven Interstellar Spacecraft?," *American Journal of Physics*, Vol. 61, No. 3, 1993, pp. 205–207. doi:10.1119/1.17291
[23] Möckel, W., "Optimum Exhaust Velocity for Laser Driven Rockets," *Journal of Spacecraft and Rockets*, Vol. 12, No. 11, 1975, pp. 700–701. doi:10.2514/3.27867
[24] Kantrowitz, A., "Propulsion to Orbit by Ground-Based Lasers," *Astronautics and Aeronautics*, Vol. 10, No. 5, 1972, pp. 74–76.
[25] Pirri, A. N., and Weiss, R. F., "Laser propulsion," AIAA 5th Fluid and Plasma Dynamics Conference, AIAA Paper 72-719, Boston, 26–28 June 1972.
[26] Bunkin, F. V., and Prokhorov, A. M., "Use of a Laser Energy Source in Producing a Reactive Thrust," *Soviet Physics, Uspekhi*, Vol. 19, No. 7, 1976, pp. 561–573. doi:10.1070/PU1976v019n07ABEH005273
[27] Ageev, V. P., Barchukov, A. I., Bunkin, F. V., Konov, V. I., Korobeinikov, V. P., Putjatin, B. V., and Hudjakov, V. M., "Experimental and Theoretical Modeling of Laser Propulsion," *Acta Astronautica*, Vol. 7, No. 1, 1980, pp. 79–90. doi:10.1016/0094-5765(80)90119-8
[28] Glumb, R. J., and Krier, H., "Concepts and Status of Laser Supported Rocket Propulsion," *Journal of Spacecraft and Rockets*, Vol. 21, No. 1, Jan.–Feb. 1984, pp. 70–79. doi:10.2514/3.8610
[29] Myrabo, L. N., Messitt, D. G., Mead, F. B., Jr., "Ground and Flight Tests of a Laser Propelled Vehicle," 36th AIAA Aerospace Science Meeting and Exhibit, AIAA Paper 98-1001, Reno, NV, 12–15 Jan. 1998.
[30] Myrabo, L. N., "World Record Flights of Beam-Riding Rocket Lightcraft: Demonstration of 'Disruptive' Propulsion Technology," 37th AIAA/ASME/ SAE/ASEE Joint Propulsion Conference, AIAA Paper 2001-3798, Salt Lake City, UT, 8–11 July 2001.
[31] Liukonen, R. A., "Laser Jet Propulsion," *XII International Symposium on Gas Flow and Chemical Lasers and High-Power Laser Conference*, Proceedings of SPIE: The International Society for Optical Engineering, Vol. 3574, SPIE, Bellingham, WA, 1998, pp. 470–474.
[32] Bohn, W. L., "Laser Lightcraft Performance," *High-Power Laser Ablation II*, Proceedings of SPIE: The International Society for Optical Engineering, Vol. 3885, SPIE, Bellingham, WA, 1999, pp. 48–53.
[33] Sasoh, A., "Laser-Driven In-Tube Accelerator," *Review of Scientific Instruments*, Vol. 72, No. 3, 2001, pp. 1893–1898. doi:10.1063/1.1347378
[34] Phipps, C. R., and Luke, J., "Diode Laser-Driven Microthrusters: A New Departure for Micropropulsion," *AIAA Journal*, Vol. 40, No. 2, 2002, pp. 310–318. doi:10.2514/2.1647
[35] Schall, W., "Orbital Debris Removal by Laser Radiation," *Acta Astronautica*, Vol. 24, 1991, pp. 343–351. doi:10.1016/0094-5765(91)90184-7; also International Astronautical Federation, Paper 90-569, 1990.
[36] Kuznetsov, L. I., and Yarygin, V. N., "Laser-Reactive Method for Disposal of Small Space Debris," *Quantum Electronics*, Vol. 24, No. 6, 1994, pp. 555–557. doi:10.1070/QE1994v024n06ABEH000138
[37] Phipps, C. R., Albrecht, G., Friedman, H., Gavel, D. D, George, E. V., Murray, J., Ho, C., Priedhorsky, W., Michaelis, M. M., and Reilly, J. P., "Orion: Clearing Near-Earth Space Debris Using a 20 kW, 530 nm, Earth-Based, Repetitively Pulsed Laser," *Laser and Particle Beams*, Vol. 14, No. 1, 1996, pp. 1–44. doi:10.1017/S0263034600009733
[38] Ageichik, A. A., Egorov, M. S., Ostapenko, S. V., Rezunkov, Y. A., Safronov, A. L., and Stepanov, V. V., "Model Test of the Aerospace Laser Propulsion Engine," *Beamed Energy Propulsion*, AIP Conference Proceedings, Vol. 766, American Inst. of Physics, Melville, NY, 2005, pp. 183–194.
[39] Phipps, C. R., and Luke, J. R., "Laser Space Propulsion," *Laser Ablation and Its Applications*, Springer, New York, 2007, pp. 407–434, Chap. 16.
[40] Pakhomov, V., and Mahaffy, K. E., "Binary Solid Propellants for Constant Momentum Missions," *Beamed Energy Propulsion*, AIP Conference Proceedings, Vol. 997, American Inst. of Physics, Melville, NY, 2008, pp. 266–279.
[41] Maesato, H., Koizumi, E., and Tahara, H., "Performance Characteristics of Low-Power Laser Ablative Thrusters for Small Satellites," *Beamed Energy Propulsion*, AIP Conference Proceedings, Vol. 830, American Inst. of Physics, Melville, NY, 2006, pp. 284–294.
[42] Schall, W. O., Eckel, H.-A., Mayerhofer, W., Riede, W., and Zeyfang, E., "Comparative Lightcraft Impulse Measurements," *High-Power Laser Ablation IV*, Proceedings of SPIE, Vol. 4760, SPIE, Bellingham, WA, 2002, pp. 908–917.
[43] Luke, J. R., and Phipps, C. R., "Laser Plasma Microthruster Performance Evaluation," *Beamed Energy Propulsion*, AIP Conference Proceedings, Vol. 664, American Inst. of Physics, Melville, NY, 2003, pp. 223–229.
[44] Phipps, C. R., Seibert, D. B. II, Royse, R., King, G., and Campbell, J. W., "Very High Coupling Coefficients at Large Laser Fluence with a Structured Target," *High Power Laser Ablation III*, edited by C. R. Phipps, Proceedings of SPIE: The International Society for Optical Engineering, Vol. 4065, SPIE, Bellingham, WA, 2000, pp. 931–938.
[45] Yabe, T., Phipps, C., Yamaguchi, M., Nakagawa, R., Aoki, K., Mine, H., Ogata, Y., Baasandash, C., Nagakawa, M., Fujiwara, E., Yoshida, K., Nishiguchi, A., and Kajiwara, I., "Micro-Airplane Propelled by Laser-Driven Exotic Target," *Applied Physics Letters*, Vol. 80, No. 23, 2002, pp. 4318–4320. doi:10.1063/1.1485313
[46] Sinko, J. E., Dhote, N. D., and Pakhomov, A. V., "Laser Propulsion with Liquid Propellants Part 2: Thin Films," *Beamed Energy Propulsion*, AIP Conference Proceedings, Vol. 997, American Inst. of Physics, Melville, NY, 2008, pp. 209–221.
[47] Phipps, C. R., Luke, J. R., and Helgeson, W., "Liquid-Fueled Laser-Powered *N*-Class Thrust Space Engine with Variable Specific Impulse," *Beamed Energy Propulsion*, AIP Conference Proceedings, Vol. 997, American Inst. of Physics, Melville, NY, 2008, pp. 222–231.
[48] Schall, W., Eckel, H.-A., and Bohn, W., "Laser Propulsion Thrusters for Space Transportation," *Laser Ablation and Its Applications*, Springer, New York, 2007, pp. 435–454.
[49] Yabe, T., Ohzono, H., Ohkubo, T., Baasandash, C., Yamaguchi, M., Oku, T., et al., "Proposal of Liquid Cannon Target Driven by Fiber Laser for Micro-Thruster in Satellite," *Beamed Energy Propulsion*, AIP Conference Proceedings, Vol. 702, American Inst. of Physics, Melville, NY, 2004, pp. 503–512.
[50] Yabe, T., Phipps, C., Aoki, K., Yamaguchi, M., Ogata, Y., Shiho, M., et al., "Laser-Driven Vehicles—From Inner-Space to Outer-Space," *High-Power Laser Ablation IV*, edited by C. R. Phipps, Vol. 4760, Proceedings of SPIE: The International Society for Optical Engineering, SPIE, Bellingham, WA, 2002, pp. 867–878.
[51] Baasandash, C., Yabe, T.,Oku, T., Ohkubo, T., Yamaguchi, M., Ohzono, H., et al., "Near-Term Application of Water-Powered Laser Propulsion," *Beamed Energy Propulsion*, AIP Conference Proceedings, Vol. 702, American Inst. of Physics, Melville, NY, 2004, pp. 513–521.
[52] Sterling, E., and Pakhomov, A. V., "Absorption-Enhanced Liquid Ablatants for Propulsion with TEA CO_2 Laser," *Beamed Energy Propulsion*, AIP Conference Proceedings, Vol. 766, American Inst. of Physics, Melville, NY, 11–14 Oct. 2004, pp. 474–481.
[53] Urech, L., Hauer, M., Lippert, T., Phipps, C. R., Schmid, E., Wokaun, A., and Wysong, I., "Designed Polymers for Laser-Based Microthrusters—Correlation of Thrust with Material, Plasma, and Shockwave Properties," *High-Power Laser Ablation V*, edited by C. R. Phipps, Proceedings of SPIE: The International Society for Optical Engineering, Vol. 5448, SPIE, Bellingham, WA, 2004, pp. 52–64.
[54] Rachuk, V. S., Guterman, V. Y., Ivanov, A. V., Rebrov, S. G., Golikov, A. N., Ponomarev, N. B., and Rezunkov, Y. A., "Experimental Investigations of Laser Propulsion by Using Gasdynamic Laser," *Beamed Energy Propulsion*, AIP Conference Proceedings, Vol. 830, American Inst. of Physics, Melville, NY, 2006, pp. 48–57.
[55] Sinko, J., and Pakhomov, A., "Delrin for Propulsion with CO_2 Laser: Carbon Doping Effects," *Beamed Energy Propulsion, Fifth International Symposium*, AIP Conference Proceedings, Vol. 997, American Inst. of Physics, Melville, NY, 2008, pp. 254–265.
[56] Grun, J., Obenschain, S., Ripin, B., Whitlock, R., McLean, E., Gardner, J., et al., "Ablative Acceleration of Planar Targets to High Velocities," *Physics of Fluids*, Vol. 26, 1983, pp. 588–597. doi:10.1063/1.864145
[57] Arad, B., Eliezer, S., Gazit, Y., Loebenstein, H., Zigler, A., Zmora, H., and Zweigenbaum, S., "Burn-Through of Thin Aluminum Foils by Laser-Driven Ablation," *Journal of Applied Physics*, Vol. 50, No. 11, 1979, pp. 6817–6821. doi:10.1063/1.325878
[58] Hatchett, S., Brown, C., Cowan, T., Henry, E., Johnson, J., Key, M., Koch, J., Langdon, A., Lasinski, B., Lee, R., Mackinnon, A., Pennington, D., Perry, M., Phillips, T., Roth, M., Sangster, T., Singh, M., Snavely, R., Stoyer, M., Wilks, S., and Yasuke, K., "Electron, Photon and Ion Beams from the Relativistic Interaction of Petawatt Laser Pulses with Solid Targets," *Physics of Plasmas*, Vol. 7,

No. 5,2000, pp. 2076–2082.
doi:10.1063/1.874030
[59] Horisawa, H., Sasaki, Y., Funaki, I., and Kimura, I., "Electromagnetic Acceleration Characteristics of a Laser-Electric Hybrid Thruster," 44th AIAA/ASME/SAE/ASEE Joint Propulsion Conference and Exhibit, AIAA Paper 2008-4818, 2008.
[60] Phipps, C. R., Reilly, J. P., and Campbell, J. W., "Optimum Parameters for Laser-Launching Objects into Low Earth Orbit," *Laser and Particle Beams*, Vol. 18, No. 4,2000, pp. 661–695.
doi:10.1017/S0263034600184101
[61] Kelly, R., and Dreyfus, R., "Reconsidering the Mechanisms of Laser Sputtering with Knudsen-Layer Formation Taken into Account," *Nuclear Instruments & Methods in Physics Research, Section B*, Vol. 32, Nos. 1–4,1988, p. 341.
doi:10.1016/0168-583X(88)90235-2
[62] Phipps, C., Jr., Turner, T., Harrison, R., York, G., Osborne, W., Anderson, G., Corlis, X., Haynes, L., Steele, H., Spicochi, K., and King, T., "Impulse Coupling to Targets in Vacuum by KrF, HF and CO_2 Lasers," *Journal of Applied Physics*, Vol. 64, No. 3,1988, pp. 1083–1096.
[63] Ihlemann, J., Beinhorn, F., Schmidt, H., Luther, K., and Troe, J., "Plasma and Plume Effects on UV Laser Ablation of Polymers," *High-Power Laser Ablation V*, edited by C. R. Phipps, Proceedings of SPIE: The International Society for Optical Engineering, Vol. 5448, SPIE, Bellingham, WA, 2004, pp. 572–580.
[64] Phipps, C., Luke, J., Moore, D., Glownia, J., and Lippert, T., "Laser Impulse Coupling at 130 fs," *Applied Surface Science*, Vol. 252, No. 13,2006, pp. 4838–4844.
doi:10.1016/j.apsusc.2005.07.079
[65] Carslaw, H., and Jaeger, J., *Conduction of Heat in Solids*, Clarendon, Oxford, 1959, p. 75.
[66] Root, R., "Modeling of Post-Breakdown Phenomena," *Laser-Induced Plasmas and Applications*, edited by L. J. Radziemski, and D. A. Cremers, Dekker, New York, 1989, pp. 78–94.
[67] Pirri, A. N., "Theory for Momentum Transfer to a Surface with a High-Power Laser," *Physics of Fluids*, Vol. 16, 1973, pp. 1435–14440.
doi:10.1063/1.1694538
[68] Raizer, Y. P., "Subsonic Propagation of a Light Spark and Threshold Conditions for the Maintenance of Plasma Radiation," *Soviet Physics, JETP*, Vol. 31, No. 31,1970, pp. 1148–1154.
[69] Beverly, R. E., III, and Walters, C. T., "Measurement of CO_2-Laser-Induced Shock Pressures Above and Below LSD-Wave Thresholds," *Journal of Applied Physics*, Vol. 47, No. 8, Aug. 1976, pp. 3485–3495.
doi:10.1063/1.323189
[70] Sinko, J., and Phipps, C., "Modeling CO_2 Laser Ablation Impulse of Polymers in Vapor and Plasma Regimes," *Applied Physics Letters*, Vol. 95, No. 13,2009, Paper 131105.
doi:10.1063/1.3234382
[71] Phipps, C., Luke, J., Lippert, T., Hauer, M., and Wokaun, A., "Micropropulsion Using Laser Ablation," *Applied Physics A: Materials Science and Processing*, Vol. 79, No. 5,2004, pp. 1385–1389.
[72] Stewart, J. E., "Infrared Spectroscopy: Experimental Methods and Techniques," *Superposition, Attenuation, and Reflection of Electromagnetic Waves*, Marcel Dekker, New York, 1970, p. 82, Chap. 3.
[73] Srinivasan, R., "Ablation of Polymers and Biological Tissue by Ultraviolet Lasers," *Science*, Vol. 234, No. 4776, 1986, pp. 559–565.
doi:10.1126/science.3764428
[74] Saha, M., "Ionization in the Solar Chromosphere," *Philosophical Magazine*, Vol. 40, 1920, p. 472.
[75] Schall, W., "Characterization of the Absorption Wave Produced by CO_2 Laser Ablation of a Solid Propellant," CR FA8655-04-1-3067 DLR, German Aerospace Center, Stuttgart, Germany, 2005.
[76] Watanabe, K., Mori, K., and Sasoh, A., "Ambient Pressure Dependence of Laser-Induced Impulse of Polyacetal," *Journal of Propulsion and Power*, Vol. 22, No. 5, 2006, pp. 1149–1151.
[77] Lippert, T., David, C., Hauer, M., Phipps, C., Wokaun, A., "Tailor-Made Polymers for Laser Applications," *Review of Laser Engineering*, Vol. 29, No. 11, 2001, p. 734.
[78] Lippert, T., David, C., Hauer, M., Wokaun, A., Robert, J., Nuyken, O., and Phipps, C., "Polymers for UV and Near-IR irradiation," *Journal of Photochemistry and Photobiology, A: Chemistry*, Vol. 145, Nos. 1–2, 2001, p. 87.
doi:10.1016/S1010-6030(01)00557-3
[79] Lippert, T., David, C., Hauer, M., Masubuchi, T., Masuhara, H., Nuyken, O., Phipps, C., Robert, J., Tada, T., Tomita, K., and Wokaun, A., "Novel Applications for Laser Ablation of Photopolymers," *Applied Surface Science*, Vol. 186, Nos. 1–4, 2002, p. 14.
doi:10.1016/S0169-4332(01)00656-0
[80] Lippert, T., Hauer, M., Phipps, C. R., and Wokaun, A., "Polymers Designed for Laser Applications: Fundamentals and Applications," *High-Power Laser Ablation IV*, Proceedings of SPIE: The International Society for Optical Engineering, Vol. 4760, SPIE, Bellingham, WA, 2002, p. 63.
[81] Lippert, T., Hauer, M., Phipps, C., and Wokaun, A., "Fundamentals and Applications of Polymers Designed for Laser Ablation," *Applied Physics A: Solids and Surfaces*, Vol. 77, No. 2, 2003, p. 259.
[82] Lippert, T., "Laser Applications of Polymers,"*Polymers and Light*, edited by T. Lippert, Advances in Polymer Science, Vol. 168, Springer, New York, 2004, pp. 51–246.
[83] Urech, L., Lippert, T., Phipps, C. R., and Wokaun, A., "Polymers as Fuel for Laser Plasma Thrusters: A Correlation of Thrust with Material and Plasma Properties by Mass Spectrometry," Proceedings of SPIE: The International Society for Optical Engineering, Vol. 6261, SPIE, Bellingham, WA, 2006, pp. 14-1–14-10.
[84] Urech, L., Lippert, T., Phipps, C. R., and Wokaun, A., "Polymers as Fuel for Laser-Based Microthrusters: An Investigation of Thrust, Material, Plasma and Shockwave Properties," *Applied Surface Science*, Vol. 253, No. 19, 2007, pp. 7646–7650.
doi:10.1016/j.apsusc.2007.02.032
[85] Urech, L., Lippert, T., Phipps, C. R., and Wokaun, A., "Polymer Ablation: From Fundamentals of Polymer Design to Laser Plasma Thruster," *Applied Surface Science*, Vol. 253, No. 15, 2007, p. 6409.
doi:10.1016/j.apsusc.2007.01.026
[86] Phipps, C. R., Luke, J. R., Lippert, T., Hauer, M., and Wokaun, A., "Micropropulsion Using a Laser Ablation Jet," *Journal of Propulsion and Power*, Vol. 20, No. 6, 2004, p. 1000.
doi:10.2514/1.2710
[87] Aoki, K., Yabe, T., Yamaguchi, M., and Baasandash, C., "Numerical and Experimental Studies of Laser Propulsion Toward Micro-Airplane," *High-Power Laser Ablation IV*, edited by C. R. Phipps, Proceedings of SPIE: The International Society for Optical Engineering, Vol. 4760, SPIE, Bellingham, WA, 2002, pp. 918–928.
[88] Zhang, Y., Lu, X., Zheng, Z. Y., Liu, F., Zhu, P. F., Li, H. M., et al., "Transmitted Laser Propulsion in Confined Geometry Using Liquid Propellant," *Applied Physics A: Solids and Surfaces*, Vol. 91, No. 2, 2008, p. 357.
doi:10.1007/s00339-008-4416-3
[89] Lippert, T., Urech, L., Fardel, R., Nagel, M., Phipps, C. R., and Wokaun, A., "Materials for Laser Propulsion: Liquid Polymers," *High-Power Laser Ablation VII*," Proceedings of SPIE: The International Society for Optical Engineering, Vol. 7005, SPIE, Bellingham, WA, 2008, pp. 12-1–12-10.
[90] Fardel, R., Urech, L., Lippert, T., Phipps, C. R., Fitz-Gerald, J. M., and Wokaun, A., "Laser Ablation of Energetic Polymer Solutions: Effect of Viscosity and Fluence on the Splashing Behavior," *Applied Physics A: Solids and Surfaces*, Vol. 94, 2009, pp. 657–665.
doi:10.1007/s00339-008-4896-1
[91] Urech, L., and Lippert, T., "Designed Polymers for Laser Ablation," *Optical Sciences*, Vol. 129, 1st ed., Springer, New York, 2007, pp. 281–297, Chap. 11.
[92] Sinko, J. E., and Pakhomov, A. V., "Laser Propulsion with Liquid Propellants Part 1: An Overview," *Beamed Energy Propulsion*, AIP Conference Proceedings, Vol. 997, American Inst. of Physics, Melville, NY, 2008, pp. 195–208.
[93] Nakano, M., Fujita, K., Uchida, S., Bato, M., and Niino, M., "Fundamental Experiments on Glycerin Propellant Laser Thruster," *Beamed Energy Propulsion*, AIP Conference Proceedings, Vol. 702, American Inst. of Physics, Melville, NY, 2004, pp. 139–145.
[94] Yamaguchi, M., Nakagawa, R., Yabe, T., Baasandash, C., Aoki, K., Ohkubo, T., et al., "Laser-Driven, Water-Powered Propulsion and Air Curtain for Vacuum Insulation," *Beamed Energy Propulsion*, AIP Conference Proceedings, Vol. 664, American Inst. of Physics, Melville, NY, 2003, pp. 557–568.
[95] Sinko, J., Kodgis, L., Porter, S., Sterling, E., Lin, J., Pakhomov, A. V., et al., "Ablation of Liquids for Laser Propulsion with TEA CO_2 Laser," *Beamed Energy Propulsion*, AIP Conference Proceedings, Vol. 830, American Inst. of Physics, Melville, NY, 2006, pp. 308–318.
[96] Sinko, J. E., "Vaporization and Shock Wave Dynamics for Impulse Generation in Laser Propulsion," Ph.D. Dissertation, Univ. of Alabama in Huntsville, Huntsville, AL, 2008.
[97] Sinko, J. E., "Time-Resolved Force and Imaging Study on the Laser Ablation of Liquids," M.S. Thesis, Univ. of Alabama in Huntsville, Huntsville, AL, 2005.
[98] Schall, W., Eckel, H.-A., and Walther, S., "Lightcraft Impulse Measurements Under Vacuum," European Office of Aerospace Research and Developement, Rept. Grant FA8655-02-M4017, London, Sept. 2002.
[99] Scharring, S., Wollenhaupt, E., Eckel, H.-A., and Röser, H.-P., "Flight

Experiments on Energy Scaling for In-Space Laser Propulsion," *Beamed Energy Propulsion* (to be published).

[100] Renz, G., Jung, M., Mayerhofer, W., and Zeyfang, E., "Pulsed CO_2-Laser with 15 kW Average Power at 100 Hz Rep-Rate," Proceedings of SPIE: The International Society for Optical Engineering, Vol. 3092, SPIE, Bellingham, WA, 1997, pp. 114–117.

[101] Myrabo, L., Libeau, M., Meloney, E., and Bracken, R., "Pulsed Laser Propulsion Performance of 11 cm Parabolic 'Bell' Engines Within the Atmosphere," 33rd Plasmadynamics and Lasers Conference, AIAA Paper 2002-2206, Maui, HI, 2002.

[102] Schall, W., Bohn, W., Eckel, H.-A., Mayerhofer, W., Riede, W., and Zeyfang, E., "Lightcraft Experiments in Germany," *Proceedings of High Power Laser Ablation III*, edited by C. R. Phipps, Proceedings of SPIE: The International Society for Optical Engineering, Vol. 4065, SPIE, Bellingham, WA, 2000, pp. 472–481.

[103] Sedov, L., *Similarity and Dimensional Methods in Mechanics*, Academic Press, New York, 1959.

[104] Ageev, V., Barchukov, A., Bunkin, F., Konov, V., Korobeinikov, V., Putjatin, B., and Hudjakov, V., "Experimental and Theoretical Modeling of Laser Propulsion," *Acta Astronautica*, Vol. 7, No. 1, 1980, pp. 79–90.
doi:10.1016/0094-5765(80)90119-8

[105] Schall, W., Eckel, H.-A., and Bohn, W., "Laser Propulsion Thrusters for Space Transportation," *Laser Ablation and Its Applications*, edited by C. R. Phipps, Springer–Verlag, New York, 2007, pp. 435–454.

[106] Scharring, S., Hoffmann, D., Eckel, H.-A., and Röser, H.-P., "Stabilization and Steering of a Parabolic Laser Thermal Thruster with an Ignition Device," *Acta Astronautica*, Vol. 65, Nos. 11–12, Dec. 2009, pp. 1599–1615.
doi:10.1016/j.actaastro.2009.04.007

[107] Ageev, V., Barchukov, A., Bunkin, F., Konov, V., Prokhorov, A., Silenok, A., and Chapliev, N., "Laser Airbreathing Jet Engine," *Soviet Journal of Quantum Electronics*, Vol. 7, 1977, pp. 1430–1437.
doi:10.1070/QE1977v007n12ABEH008257

[108] Bohn, W., and Schall, W., "Laser Propulsion Activities in Germany," *Beamed Energy Propulsion*, AIP Conference Proceedings, Vol. 664, American Inst. of Physics, Melville, NY, 2003, pp. 79–91.

[109] Eckel, H.-A., and Schall, W., "Laser Propulsion Systems," *Advanced Propulsion Systems and Technologies, Today to 2020*, edited by C. Bruno, and A. G. Accettura, Progress in Astronautics and Aeronautics, AIAA, Reston, VA, 2008, pp. 357–406.

[110] Eckel, H.-A., Tegel, J., and Schall, W., "CO_2 Laser Absorption in Ablation Plasmas," *Beamed Energy Propulsion*, AIP Conference Proceedings, Vol. 830, American Inst. of Physics, Melville, NY, 2005, pp. 272–283.

[111] Pakhomov, A., and Mahaffy, K., "Binary Solid Propellants for Constant Momentum Missions," *Beamed Energy Propulsion*, AIP Conference Proceedings, Vol. 997, American Inst. of Physics, Melville, NY, 2008, pp. 266–279.

[112] Scharring, S., Eckel, H.-A., and Röser, H.-P., "Flight Analysis of a Parabolic Lightcraft—Ground-Based Launch," *Beamed Energy Propulsion*, AIP Conference Proceedings, Vol. 997, American Inst. of Physics, Melville, NY, 2008, pp. 304–315.

[113] Hoffmann, D., "Development And Validation Of A Design Model with Remotely Controllable Steering Gear for Flight Experiments on Pulsed Laser Thermal Propulsion," Diplom. Thesis, Inst. of Space Systems, Univ. of Stuttgart, 2008.

[114] Sinko, J., Dhote, N., Lassiter, J., and Gregory, D., "Conical Nozzles for Pulsed Laser Propulsion," *High-Power Laser Ablation VII*, Proceedings of SPIE: The International Society for Optical Engineering, Vol. 7005, SPIE, Bellingham, WA, 2008, pp. 2Q1–2Q10.

[115] Vinogradov, B., Perepelkin, K., and Mechsheriakova, G., *Laser Radiation Effects on Polymers*, Vols. 1, 2, Nauka, St. Petersburg, Russia, 2006.

[116] Eremenko, L., and Nesterenko, D., *Chemistry of Detonation. Production of Detonation Waves by Explosives of Various Atomic Composition*, Russian Academy of Sciences, Inst. of Chemical Physics, Chernogolovka, Russia, 1992, p. 11.

[117] Aseev, E., and Zaikov, E., *Burning of Polymers*, Nauka, Moscow, 1981, p. 280.

[118] Ageichik, A., Repina, E., Rezunkov, Y., and Safronov, A., "Detonation of CHO Working Substances in a Laser Jet Engine," *Technical Physics*, Vol. 54, No. 3, March 2009, pp. 402–409.
doi:10.1134/S1063784209030128

[119] Phipps, C. R., Luke, J. R., Helgeson, W., and Johnson, R., "A ns-Pulse Laser Microthruster," *Beamed Energy Propulsion*, AIP Conference Proceedings, Vol. 830, American Inst. of Physics, Melville, NY, 2006, pp. 235–246.

[120] Phipps, C., and Luke, J., "Feasibility of a 5-Millinewton Laser Minithruster," NASA John H. Glenn Research Center at Lewis Field, CR NNC07QA25P, Cleveland, OH, 2007.

[121] Hertzberg, A., Bruckner, A., and Bogdanoff, D., "Ram Accelerator: A New Chemical Method for Accelerating Projectiles to Ultrahigh Velocities," *AIAA Journal*, Vol. 26, No. 2, 1988, pp. 195–203.
doi:10.2514/3.9872

[122] Knowlen, C., and Bruckner, A., "A Hugoniot Analysis of the Ram Accelerator," *Proceedings of the 18th International Symposium on Shock Waves*, Springer–Verlag, Berlin, 1992, pp. 617–622.

[123] Bruckner, A., "The Ram Accelerator: Overview and State of the Art," *Ram Accelerators*, edited by K. Takayama, and A. Sasoh, Springer–Verlag, Heidelberg, Germany, 1998, pp. 1–23.

[124] Sasoh, A., Urabe, N., and Kim, S., "Impulse Enhancement by In-Tube Operation in Laser Propulsion," *High-Power Laser Ablation IV*, Proceedings of SPIE, Vol. 4760, SPIE, Bellingham, WA, 20082002, pp. 879–886.

[125] Sasoh, A., Urabe, N., Kim, S., and Jeung, I.-S., "Impulse Dependence on Propellant Condition in a Laser-Driven In-Tube Accelerator," *Transactions of the Japan Society for Aeronautical and Space Sciences*, Vol. 48, No. 160, 2005, pp. 63–70.
doi:10.2322/tjsass.48.63

[126] Sasoh, A., Suzuki, S., Shimono, M., and Sawada, K., "Moderate-Acceleration Launch Using Repetitive-Pulse Laser Ablation in a Tube," *Journal of Propulsion and Power*, Vol. 24, No. 5, 2008, pp. 1144–1146.
doi:10.2514/1.36168

[127] Sasoh, A., Suzuki, S., and Matsuda, A., "Wall-Propelled, In-Tube Propulsion with Repetitive-Pulse Laser Ablation," *Journal of Propulsion and Power*, Vol. 25, No. 2, 2009, pp. 540–542.
doi:10.2514/1.39999

[128] Anju, K., Sawada, K., Sasoh, A., Mori, K., and Zaretsky, E., "Time-Resolved Measurements of Impulse Generation in Pulsed Laser-Ablative Propulsion," *Journal of Propulsion and Power*, Vol. 24, No. 2, 2008, pp. 322–329.
doi:10.2514/1.32017

[129] Suzuki, K., Sawada, R., Takaya, R., and Sasoh, A., "Ablative Impulse Characteristics of Polyacetal with Repetitive CO_2 Laser Pulses," *Journal of Propulsion and Power*, Vol. 24, No. 4, 2008, pp. 834–841.
doi:10.2514/1.32477

[130] Horisawa, H., Kawakami, M., Lin, W.-W., Igari, A., and Kimura, I., "Discharge Characteristics of a Laser-Assisted Plasma Thruster," 28th International Electric Propulsion Conference, Paper IEPC 03-0075, 2003.

[131] Horisawa, H., Igari, A., Kawakami, M., and Kimura, I., "Discharge Characteristics of Laser-Electric Hybrid Thrusters," 40th AIAA/ASME/SAE/ASEE Joint Propulsion Conference and Exhibit, AIAA Paper 2004-3937, 2004.

[132] Horisawa, H., Kawakami, M., and Kimura, I., "Laser-Assisted Pulsed Plasma Thruster for Space Propulsion Applications," *Applied Physics A: Solids and Surfaces*, Vol. 81, No. 2, 2005, pp. 303–310.
doi:10.1007/s00339-005-3210-8

[133] Horisawa, H., Sasaki, Y., Funaki, I., and Kimura, I., "Electromagnetic Acceleration Characteristics of a Laser-Electric Hybrid Thruster," 44th AIAA/ASME/SAE/ASEE Joint Propulsion Conference and Exhibit, AIAA Paper 2008-4818, 2008.

[134] Ono, T., Uchida, Y., Horisawa, H., Funaki, I., "Measurement of Ion Acceleration Characteristics of a Laser-Electrostatic Hybrid Microthruster for Space Propulsion Applications," *Vacuum*, Vol. 83, No. 1, 2008, pp. 213–216.
doi:10.1016/j.vacuum.2008.03.098

[135] Umstadter, D., "Review of Physics and Applications of Relativistic Plasmas Driven by Ultra-Intense Lasers," *Physics of Plasmas*, Vol. 8, No. 5, 2001, pp. 1774–1785.
doi:10.1063/1.1364515

[136] Tajima, T., and Mourou, G., "Zetawatt-Exawatt Lasers and Their Applications in Ultrastrong-Field Physics," *Physical Review Special Topics*, Vol. 5, 2002, Paper 031301.
doi:10.1103/PhysRevSTAB.5.031301

[137] Snavely, R., Key, M., Hatchett, S., Cowan, T., Roth, M., Phillips, T., et al., "Intense High-Energy Proton Beams from Petawatt-Laser Irradiation of Solids," *Physical Review Letters*, Vol. 85, No. 14, 2000, pp. 2945–2948.
doi:10.1103/PhysRevLett.85.2945

[138] Sentoku, Y., Liseikina, T., Esirkepov, T., Califano, F., Naumova, N., Ueshima, Y., et al., "High Density Collimated Beams of Relativistic Ions Produced by Petawatt Laser Pulses in Plasmas," *Physical Review E (Statistical Physics, Plasmas, Fluids, and Related Interdisciplinary Topics)*, Vol. 62, No. 5, 2000, pp. 7271–7281.
doi:10.1103/PhysRevE.62.7271

[139] Horisawa, H., and Kimura, I., "Characterization of Novel Laser Accelerators for Space Propulsion," 36th AIAA/ASME/SAE/ASEE Joint Propulsion Conference and Exhibit, AIAA Paper 2000-3487, 2000.

[140] Horisawa, H., Kuramoto, H., Emura, H., Uchida, N., and KIMURA, I., "A Relativistic Laser-Accelerated Plasma Thruster for Space Propulsion," 38th AIAA/ASME/SAE/ASEE Joint Propulsion Conference and Exhibit, AIAA Paper 2002-3780, 2002.

[141] Horisawa, H., Kuramoto, H., Oyaizu, K., Uchida, N., and Kimura, I., "Fundamental Study of a Relativistic Laser-Accelerated Plasma Thruster," *Beamed Energy Propulsion*, AIP Conference Proceedings, Vol. 664, American Inst. of Physics, Melville, NY, 2003, pp. 411–422.

[142] Horisawa, H., and Kimura, I., "A Very-High-Specific-Impulse Relativistic Laser Thruster," *Beamed Energy Propulsion*, AIP Conference Proceedings, Vol. 997, American Inst. of Physics, Melville, NY, 2008, pp. 561–571.

[143] Rashleigh, S., and Marshall, R., "EM Acceleration of Macroparticles to High Velocity," *Journal of Applied Physics*, Vol. 49, No. 4, 1978, pp. 2540–2542.
doi:10.1063/1.325107

[144] McNab, I., "Launch to Space with an Electromagnetic Railgun," *IEEE Transactions on Magnetics*, Vol. 39, No. 1, 2003, pp. 295–304.
doi:10.1109/TMAG.2002.805923

[145] McNab, I., "Progress on Hypervelocity Railgun Research for Launch to Space," *IEEE Transactions on Magnetics*, Vol. 45, No. 1, 2009, pp. 381–388.
doi:10.1109/TMAG.2008.2008601

[146] Mead, F., Jr., Larson, C., and Knecht, S., "An Overview of the Experimental 50 cm Laser Ramjet (X-50LR) Program," *Beamed Energy Propulsion*, AIP Conference Proceedings, Vol. 830, American Inst. of Physics, Melville, NY, 2005, pp. 534–552.

[147] Larson, C., Mead, F., Jr., and Kalliomaa, W., "Energy Conversion in Laser Propulsion 3," *Beamed Energy Propulsion*, AIP Conference Proceedings, Vol. 664, American Inst. of Physics, Melville, NY, 2003, pp. 170–181.

[148] Knecht, S., Mead, F., Jr., Micci, M., and Larson, C., "Trajectory Simulations, Qualitative Analyses and Parametric Studies of A Laser-Launched Micro-Satellite Using OTIS," *Beamed Energy Propulsion*, AIP Conference Proceedings, Vol. 830, American Inst. of Physics, Melville, NY, 2005, pp. 522–533.

[149] Wang, T.-S., Chen, Y.-S., Liu, J., Myrabo, L., and Mead, F., Jr., "Advanced Performance Modeling of Experimental Laser Lightcraft," *Journal of Propulsion and Power*, Vol. 18, No. 6, 2002, pp. 1129–1138.
doi:10.2514/2.6054

[150] Komurasaki, K., Arakawa, Y., Hosoda, S., Katsurayama, H., and Mori, K., "Fundamental Researches on Laser Powered Propulsion," 33rd Plasmadynamics and Lasers Conference, AIAA Paper 2002-2200, May 2002.

[151] Katsurayama, H., Komurasaki, K., and Arakawa, Y., "Numerical Analyses on Pressure Wave Propagation in Repetitive Pulse Laser Propulsion," 37th Joint Propulsion and Conference, AIAA Paper 2001-3665, July 2001.

[152] Minucci, M., Toro, P., Chanes, J., Jr., Ramos, A., Pereira, A., Nagamatsu, H., and Myrabo, L., "Investigation of a Laser-Supported Directed-Energy 'Air Spike' in Hypersonic Flow—Preliminary Results," *Journal of Spacecraft and Rockets*, Vol. 40, No. 1, 2003, pp. 133–135.
doi:10.2514/2.3927

[153] Minucci, M. A. S., Toro, P. G. P., Oliveira, A. C., Ramos, A. G., Chanes, J. B., Jr., Pereira, A. L., Nagamatsu, H. T., Myrabo, L. N., "Laser-Supported Directed-Energy 'Air Spike' Hypersonic Flow," *Journal of Spacecraft and Rockets*, Vol. 42, No. 1, 2005, pp. 51–57.
doi:10.2514/1.2676

[154] Oliveira, A., Minucci, M.,Toro, P., Channes, J. B., Jr., and Salvador, I., "Schilieren Visualization Technique Applied to the Study of laser–plasma Induced Breakdown in Low Density Hypersonic Flow," *Beamed Energy Propulsion*, AIP Conference Proceedings, Vol. 830, American Inst. of Physics, Melville, NY, 2005, pp. 504–509.

[155] Salvador, I., Minucci, M., Toro, P., Oliveira, A., Channes, J., Jr., Myrabo, L., and Nagamatsu, H., "Experimental Analysis of Heat Flux to a Blunt Body in Hypersonic Flow with Upstream Laser Energy Deposition—Preliminary Results," *Beamed Energy Propulsion*, AIP Conference Proceedings, Vol. 830, American Inst. of Physics, Melville, NY, 2005, pp. 163–171.

[156] Rezunkov, Y., Safronov, A., Ageichik, A., Egorov, M., Stepanov, V., Rachuk, V., et al., "Performance Characteristics of Laser Propulsion Engine Operating Both in CW and in Repetitively Pulsed Modes," *Beamed Energy Propulsion*, AIP Conference Proceedings, Vol. 830, American Inst. of Physics, Melville, NY, 2006, pp. 3–12.

[157] Liukonen, R. A., and "Efficiency of the Laser Power Transformation into Mechanical Impulse in Laser Propulsion Engine," *JETP Letters*, Vol. 18, 1992, pp. 76–79.

[158] *Chemistry Encyclopedia*, Soviet Encyclopedia Publishing, Moscow, 1988.

[159] Ageichik, A., Egorov, M., Rezunkov, Y., Safronov, A., and Stepanov, V., "Aerospace Laser Propulsion Engine," Russian Patent Application No. 2003129824, filed 8 Oct. 2003.

[160] Ageichik, A., Egorov, M., Ostapenko, S., Rezunkov, Y., Safronov, A., and Stepanov, V., "Model Tests of Aerospace Laser Propulsion Engine," *Beamed Energy Propulsion*, AIP Conference Proceedings, Vol. 766, American Inst. of Physics, Melville, NY, 2004, pp. 183–194.

[161] Rezunkov, Y., Sirazetdinov, V., Starikov, A., and Charukhchev, A., "Simulation of High-Power Physical Processes by Using Multipurpose Lasers," *Journal of Optical Technology*, Vol. 61, No. 1, 1994, pp. 68–76.

[162] Raizer, Y., *Laser-Induced Discharge Phenomena*, Consultants Bureau, New York, 1977, pp. 198–249.

[163] di Teodoro, F., "Megawatt Peak-Power Pulsed Fiber Sources," *High-Power Laser Ablation VI*, Proceedings of SPIE: The International Society for Optical Engineering, Vol. 6261, SPIE, Bellingham, WA, 2006, pp. 1N-1–1N-8.

[164] Phipps, C., "LISK-BROOM: A Laser Concept for Clearing Space Junk," *Laser Interaction and Related Plasma Phenomena*, AIP Conference Proceedings, Vol. 318, American Inst. of Physics, Melville, NY, 1994, p. 466–468.

[165] Schall, W., "Laser Radiation for Clearing Space Debris from Lower Earth Orbit," *Journal of Spacecraft and Rockets*, Vol. 39, No. 1, 2002, pp. 81–91.
doi:10.2514/2.3785

[166] Campbell, J. W., "Project Orion: Orbital Debris Removal Using Ground-Based Sensors and Lasers," NASA TM 108522, 1996.

[167] Phipps, C., "Orion: Challenges and Benefits," *High-Power Laser Ablation I*, edited by C. R. Phipps, Proceedings of SPIE: The International Society for Optical Engineering, Vol. 3343, SPIE, Bellingham, WA, 1998, pp. 575–582.

[168] Phipps, C., "Ultrashort Pulses for Impulse Generation in Laser Propulsion Applications," *Laser Interactions and Related Plasma Phenomena*, AIP Conference Proceedings, Vol. 406, American Inst. of Physics, Melville, NY, 1997, pp. 477–484.

[169] "Space Settlements: A Design Study," edited by R. D. Johnson, and C. Holbrow, NASA Rept. SP-413, 1977.

[170] Phipps, C., "Conceptual Design of a 170-MJ Hydrogen Fluoride Laser for Fusion," *Laser and Particle Beams*, Vol. 7, No. 4, 1989, p. 835.
doi:10.1017/S0263034600006297

[171] Sänger, E., "Flight Mechanics of Photon Rockets," *Aero Digest*, Vol. 73, No. 1, July 1956, pp. 68–73.

G. Spanjers
Associate Editor